FORSCHUNGSBERICHT AGRARTECHNIK
des Arbeitskreises Forschung und Lehre der
Max-Eyth-Gesellschaft Agrartechnik im VDI (VDI-MEG) **602**

Florian Balbach

Load based evaluation of machines using the example of a tractor

Dissertation Hohenheim 2018

Load based evaluation of machines using the example of a tractor

Von der Fakultät Agrarwissenschaften
der Universität Hohenheim
zur Erlangung des Grades eines Doktors der Agrarwissenschaften
(Dr.sc.agr.)
genehmigte Abhandlung

vorgelegt

von
M.Sc. Florian Balbach
aus Stuttgart, Baden-Württemberg

Hauptberichter:	Prof. Dr.-Ing. S. Böttinger
Mitberichter:	Prof. Dr. H. Korte
Tag der mündlichen Prüfung:	25.10.2018

Institut für Agrartechnik
Stuttgart 2018

Florian Balbach

Load based evaluation of machines using the example of a tractor

D 100 (Diss. Universität Hohenheim)

Shaker Verlag
Aachen 2019

Bibliographic information published by the Deutsche Nationalbibliothek
The Deutsche Nationalbibliothek lists this publication in the Deutsche Nationalbibliografie; detailed bibliographic data are available in the Internet at http://dnb.d-nb.de.

Zugl.: Hohenheim, Univ., Diss., 2018

Printed in Germany.

ISBN 978-3-8440-6408-7
ISSN 0931-6264

Shaker Verlag GmbH • P.O. BOX 101818 • D-52018 Aachen
Phone: 0049/2407/9596-0 • Telefax: 0049/2407/9596-9
Internet: www.shaker.de • e-mail: info@shaker.de

Vorwort

Die vorliegende Arbeit entstand im Rahmen einer Industriepromotion in Zusammenarbeit mit dem Fachbereich Grundlagen der Agrartechnik am Institut für Agrartechnik der Universität Hohenheim und dem Bereich Produktstrategie der Firma CLAAS aus Harsewinkel.

Allen voran danke ich Herrn Dr. Eberhard Nacke, welcher mich Ende 2014 mit an Bord der Firma CLAAS holte und mir während der gesamten Zeit mit hervorragenden Ideen und Anregungen zur Seite stand. Zusammen mit den Herren Jan Wieckhorst und Christian Ehlert entstand aus einer Laune am Rande eines Workshops die grundsätzliche Idee für die vorliegende Arbeit.

Großen Dank möchte ich auch an Herrn Prof. Dr.-Ing. Stefan Böttinger aussprechen, welcher mir als Doktorvater stets mit seiner wissenschaftlichen Erfahrung und fachlichen Expertise zur Seite stand. Seine zahlreichen Ratschläge und Anregungen haben wesentlich zum Gelingen meiner Arbeit beigetragen.

Herrn Prof. Dr. Hubert Korte möchte ich an dieser Stelle für seine Begeisterung und Überzeugung für mein Thema, seine praxisorientierten Impulse, sowie für die Durchsicht der Arbeit und die Übernahme des Mitberichts danken.

Viele Kollegen haben mich im Laufe der Arbeit mit Ihrem Wissens- und Erfahrungsschatz unterstützt. Im Besonderen möchte ich Frau Carolin Hammacher, sowie den Herren Dr. Thomas Fedde, Klaus Ellermann, Christian Birkmann, Michael Peeters und Sebastian Stellmach aus den Bereichen Traktor Entwicklung, Traktor Vorentwicklung und Validierung danken.

Eine besondere Erwähnung verdient Herr Christopher Fender, welcher als Native Speaker mit großer Motivation meine Arbeit in mancher Nachtschicht im Englischen feingeschliffen hat.

Danken möchte ich auch meinen Eltern Ingrid und Rainer Balbach, welche mich immer in meinen Vorhaben bestärkt und unterstützt haben, sowie Anna, meiner treuen Partnerin in allen Lebenslagen.

Ravensburg, im November 2018 *Florian Balbach*

CONTENT

FORMULA SYMBOLS

D	Damage	
G	Tractor gross weight	N
L	Load sum	
LF	Load factor	
LR	Load ratio	
M	Torque	Nm
N	Number of load cycles	
P	Power	kW
R	Resistance	Ω
S	Stress	
U	Voltage	V
c	Factor for crack growth	
e	Exponent c.f. Fig. 10 and Eq.(7)	
k	Exponent of finite life straight	
m	Mass	kg
n	Actual number of load cycles	
r	Radius	m
t	Time/function of time	
κ	Net traction ratio	
μ	Circumference coefficient	
ρ	Roll resistance	

INDICES

A	Support voltage
B	Measuring signal
D	Point of endurance
E	Engine

a	Level of a specific stress amplitude
i	Index of load class
max	Maximum/gross weight
net	Net weight
o	Index of highest load class

ABBREVIATIONS

AC	Air conditioner
ATV	All terrain vehicle
BMELV	Federal Ministry of Food and Agriculture
CAN	Controller area network
CAT	Caterpillar
CM	Condition monitoring
CNH	Case - New Holland
CVT	Continuous variable transmission
DESTATIS	Statistisches Bundesamt (Federal Statistical Office Germany)
DIN	Deutsches Institut für Normung (German Institute for Standardization)
DLG	Deutsche Landwirtschafts-Gesellschaft (German Agriculture Society)
ECE	Economic Commission for Europe
ECU	Electronic control unit
EL	Engine load
ERL	Estimation of remaining lifetime
FC	Fuel consumption
FKM	Forschungskuratorium Maschinenbau (Research Curatorship for Mechanical Engineering)
GPS	Global positioning system
ICE	Intercity-Express
ISO	International Organization for Standardization
KBA	Kraftfahrt Bundesamt (Federal Motor Transport Authority)

KTBL	Kuratorium für Technik und Bau in der Landwirtschaft (Curatorship for Technology and Construction in Agriculture)	
MFWD	Mechanical front wheel assist	
OEM	Original equipment manufacturer	
PM	Predictive maintenance	
PTO	Power take-off	
ROH	Real operation hours	
RPM	Revolutions per minute	
SDF	Same Deutz-Fahr	
SG	Summer barley	
TCO	Total cost of ownership	
US	United States	
VDMA	Verband Deutscher Maschinen- und Anlagenbau (German Engineering Federation)	
VOH	Weight factor of operation hours	
WR	Winter canola (rapeseed)	
WW	Winter wheat	
avg.	Average	Ø
bn	Billion ($*10^9$)	
cf.	Compare with	
h	Hours	
ha	Hectare	
k€	Thousand Euros ($*10^3$)	€
w	with	
w/o	without	

ABSTRACT

The estimation of tractor value requires a lot of experience and knowledge and relies mainly on total operation hours and manufacturing year. Today each tractor operation hour is considered to be equal because tractor meters operate time based only and do not consider the varying loads. But tractors face multiple applications within a year. Each application puts different loads on each tractor assembly such as engine, gearbox, axles or power take-off.

A more precise method is introduced to evaluate tractor operation hours on basis of real application loads of each tractor assembly within the drivetrain separately. The method relates accumulated tractor loads to standard operation loads which are defined by a reference load spectrum for the specific assembly. For the load evaluation a pseudo damage calculation similar to the Miner's rule is used.

A test tractor was equipped with strain gauge sensors to measure torque flow within the drivetrain. A variety of different tractor applications were measured and load spectra for different assemblies were generated. Based on different tractor application profiles lifetime load spectra for the different assemblies can be calculated. Further consolidation of the individual load factors can be done by weighting of the assemblies. The resulting load factor brings transparent information about intensity of tractor usage. Results show big differences between the assemblies and between the different application profiles. This supports the demand for a new method for tractor evaluation.

1 INTRODUCTION

Agriculture is facing structural change all over the world. Especially in developed countries the number of actual farms and farmers is decreasing while the farms themselves become bigger and bigger. The type of farms are changing with the size as well, from small family farming operations to giant corporate farms which are managed like companies. The more professionalization there is, the more transparency is demanded by buyers of agricultural machinery. Structural change forces the farms to focus more on specialization. This also has an effect on the agricultural machinery used, especially the tractor's role as central and universal work machine. The annual application spectrum of a tractor depends on a variety of factors such as farm type or farm size, among others. This means that tractors are used as multipurpose machines with low annual application hours per application or as single purpose machine with high annual usage, depending on the level of specialization of the farms. Machine idle time differs greatly as well. While most tractors have 25 - 30 % idle in their load spectrum, individual machines can have below 20 % or above 35 % idle time [1; 2].

Every tractor application puts loads on different tractor assemblies such as engine, gearbox or axles. Nowadays a simple hour meter is the basis for tractor evaluation and tractor service. In the past tractors were equipped with so called "tractor meters", shown in **Figure 1**. These devices were driven manually by the engine crankshaft. Depending on the engine speed these tractor meters counted less "hours" for one hour at engine idle speed in comparison to one hour of engine nominal speed. The hint "1 maintenance hour equals 1 hour at 1,500 min^{-1} engine speed" was written on some of these tractor meters. Assuming a relation between engine load and RPM the tractor meters weighted tractor operation somehow based on tractor load. Although this practice is still well known today, now time-based operation hours are used for tractor evaluation. Approaches like condition monitoring are used for critical infrastructure or machines with demand for high uptime rate to monitor actual condition. This is mostly done on basis of vibro-acoustic sensors which have to be installed separately and must be calibrated individually on the machine. Because the costs of these systems are quite high other approaches like load prediction or out-of-spec monitoring based on operational data were established but do not fulfill the requirements of a modern tractor meter [3; 4].

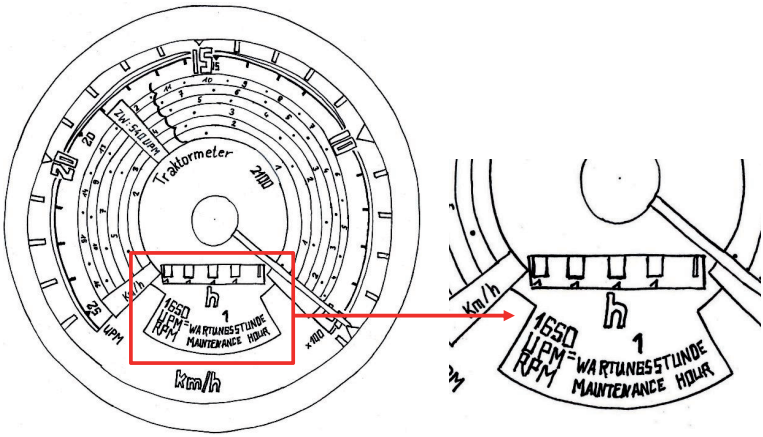

Figure 1: Historical tractor meter for Deutz tractors, with reference to maintenance hour, 1960s.

This demands a new method which evaluates single tractors on the basis of actual loads within the drivetrain. The evaluation should be kept separately for the different tractor assemblies like engine, gearbox input and output side, front and rear axle and perhaps the power take-off (PTO). The result should bring more transparency to tractor load history and actual cumulated loads on the assemblies. In order to evaluate the whole tractor, combining of the assembly-specific loads into one encompassing load factor should be possible. False estimates of impending tractor failure must be avoided because they reduce the credibility of the system. Evaluation of the whole tractor is necessary to make an evaluation of tractor usage or residual value. The system can be used for tractor validation, evaluation of the economy of tractor usage or used-machinery, and can help to establish load-specific maintenance intervals.

2 LITERATURE REVIEW

2.1 Market aspects and tractor usage

The German tractor market sales in 2017, as shown in **Table 1**, was just over 26,000 units, down from almost 28,500 units in 2016. Depending on the defined kW-range, the largest manufacturers are John Deere, Fendt, Same Deutz-Fahr (SDF), CLAAS and Case-New Holland (CNH). Worldwide revenue in the agricultural machinery business in 2012 was 91 bn € while tractors accounted for 40 bn € [5].

Table 1: German market share of the larger tractor manufacturers, registrations until November 2017; from [5].

	2017		2016	
Manufacturer	**Units**	**Market share %**	**Units**	**Market share %**
John Deere	5,286	20.3	5,222	18.3
Fendt	5,172	19.8	4,602	16.2
Deutz-Fahr	2,039	7.8	2,743	9.6
Kubota	1,921	7.4	2,021	7.1
CLAAS	1,871	7.2	2,048	7.2
Case IH/ Steyer	1,715	6.6	2,391	8.4
New Holland	1,502	5.8	1,970	6.9
Massey Fergusson	877	3.4	1,156	4.1

Table 2: German tractor market (total market), production not including North America from VDMA [6], exports without used machinery from DESTATIS [7], registrations and changing owner excluding ATV and telescopic handlers from KBA [8].

Year	**2010**	**2011**	**2012**	**2013**	**2014**	**2015**	**2016**
Production	50,865	60,551	59,213	63,599	51,349	39,340	35,926
Registrations	28,587	35,977	36,264	36,248	34,611	32,220	28,248
Exports	43,959	51,594	49,808	53,898	47,135	46,881	41,456
Changing owner	93,084	96,597	95,005	99,468	102,217	103,015	117,765

At the same time the number of used tractor market, which shall be indicated by “changing owner” in **Table 2** is 2 - 3 times the size of the new tractor sales. This gives significant importance to this aspect of the market and asks for the question of important cost factors for tractors.

An analysis of Renius, **Figure 2**, shows distribution of tractor operation costs (55 kW) based on the annual operation hours from the year 1976. Depreciation contributes significant to the high fixed costs. The author mentions that the general indication of the plot is still relevant but costs for interest rates and maintenance have decreased slightly and costs for operating material increased [9].

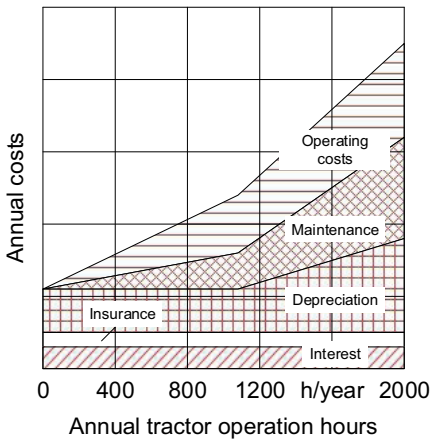

Figure 2: Total cost of tractor ownership, based on annual operation hours; [9].

An analysis of the German used tractor market indicates that the calculated costs for depreciation, which on the one hand are set by German tax authorities (depreciation over 8 years) and on the other hand still depend on the resale value on the used tractor market.

Figure 3 shows the used machinery market for John Deere, Fendt, CLAAS and Deutz-Fahr tractors in the 130 kW segment on the German online trading platform for agricultural machinery, “technikboerse”. The analysis shows the listed prices, based on

operation hours and tractor age. The exponential fitted trend curves are highly influenced by tractor operation hours. When taking older tractors with higher operation hours into consideration a higher impact of tractor age can be observed. This means that from a customer's point of view resale value of a tractor plays an important role when determining total cost of ownership (TCO).

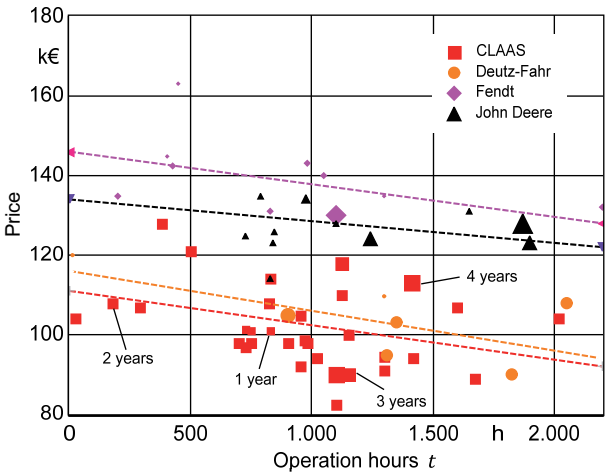

Figure 3: Used machinery market for tractors within the 130 kW range, n = 61 units from online trading platform technikbörse, size of symbols indicates tractor age.

Akerlof once established the idea of new and used cars in the category of good and bad cars (so-called lemon cars). He assumes that "owners, after using the car for a length of time can form a good idea whether it is a good car or a lemon". This leads in his opinion to the situation that most used cars sold will be lemons [10]. However assuming the tractor manufacturer wants to provide sufficient and continuous quality the usage of a tractor will have a huge impact on being a "good" tractor or a "lemon".

Figure 4 shows cumulated annual application time of mechanical front wheel drive tractors (MFWD) in western Germany, in 1994, over tractor nominal power. With increasing tractor power the portion of tillage also increases, while the other application

types decrease. The author mentions that the general distribution is still valid today, but tractor power has increased [11].

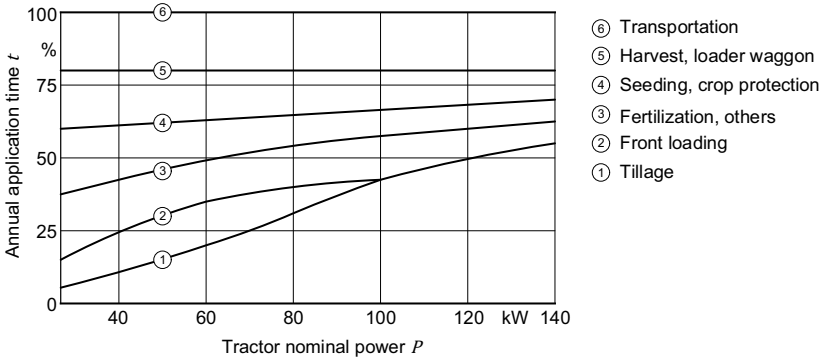

Figure 4: Annual application times for MFWD tractors in western Germany in 1994 as stacked diagram, farm size 50 - 100 ha; [11].

Calculated tractor lifetime is estimated to 10,000 operation hours [12]. The observed lifetime is often higher than 10,000 operation hours. Welschoff mentions the slightly changing usage with increasing tractor age as a reason for this phenomenon [13]. At the end of the tractor's lifecycle they are used for lighter applications which put less load on the tractor drivetrain assemblies. This results in higher operation hours than under the assumed application spectrum. Approaches to evaluating these operational loads and predicting remaining lifetime are shown in chapter **2.3**. But it has to be mentioned that prediction of loads or prediction of the remaining lifetime (which needs an assumption of future tractor application ratio) is difficult or impossible because of the seasonal and lifetime shift in tractor usage.

2.2 Load aspects

2.2.1 Concept of fatigue

Machine design is always a compromise between durability and lightweight construction. This conflict exists especially for mobile machines such as agricultural machinery or planes [14]. It led to the concept of fatigue strength which covers vibration resistance, mostly periodic loads such as waves, and operational stability which consist of stochastic or deterministic load sequences.

Operational stability is a lifetime-oriented approach. It is based on real operational loads. The basics of fatigue strength testing lead back to August Wöhler. He developed a procedure for testing standardized material samples by stress with periodic loads. During the Wöhler fatigue test, the number of load cycles until failure of the sample and magnitude of load amplitude are plotted against each other. A repetition at other load levels result in the Wöhler curve, shown in **Figure 5**.

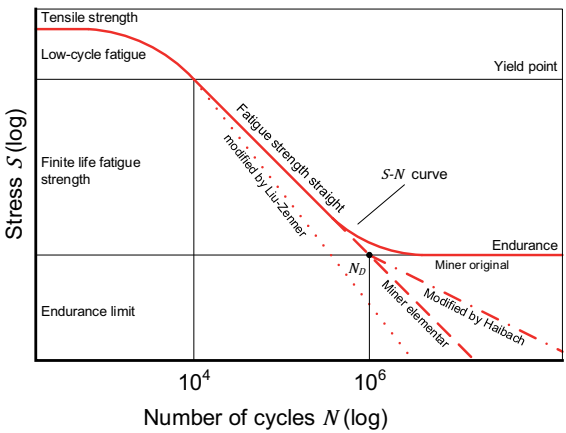

Figure 5: Specific areas of a theoretical Wöhler curve and different damage accumulation hypotheses in double-logarithmic plot; edited from [14].

The Wöhler curve is characterized by the area of low-cycle fatigue $N \leq 10^4$ cycles and finite life fatigue strength $10^4 < N \leq 10^5$ cycles. The knee point to endurance is usually

at $N_D = 10^6$ - 10^7. The upper part of the Wöhler curve can be reduced to a horizontal line at the level of static strength of the probe. This point is usually between 10 - 1,000 cycles. According to Radaj, the Wöhler curve can be generalized and load amplitude can be defined by global stress parameters [14]. Exemplary Wöhler curves for different components and a load spectrum are shown in **Figure 6**.

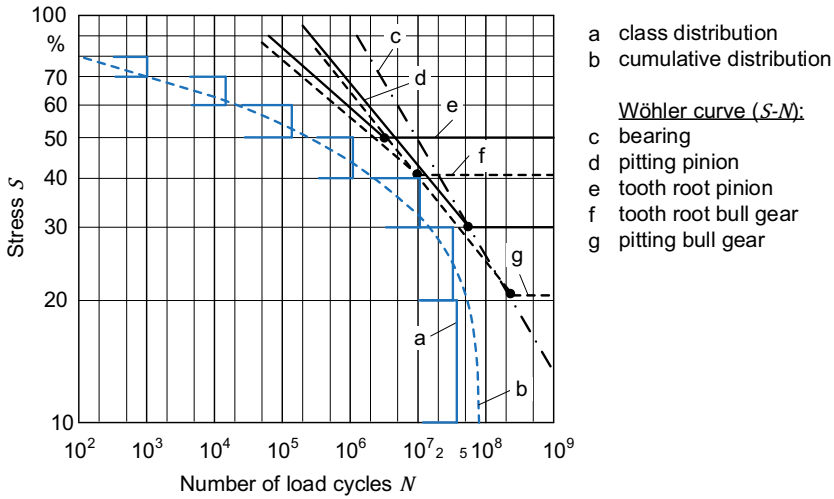

Figure 6: Miner's rule - calculation procedure of damage accumulation hypothesis, load spectrum in cumulative and class distribution and in black different Wöhler curves for specific assemblies.

To calculate remaining lifetime of a component, based on real loads or load spectrum, so called damage accumulation hypothesis have been established. These are categorized in linear, non-linear and relative methods [15]. Linear damage accumulation methods are mostly used for agricultural machine development. These assume load amplitudes with the same magnitude cause equal damage. Frequency and sequence of loads are considered to be irrelevant.

For calculation of damage, according to linear damage accumulation hypothesis load spectrum (cumulative frequencies) is divided into classes with constant load amplitudes S_a (relative frequencies). For each single class, a number of load cycles n_i is assigned. Damage is calculated by the ratio of maximum potential of load cycles N_i and actual load cycles n_i in this class. N_i is defined by one-phase Wöhler test. A components accumulated damage is calculated by **Eq.(1)**. If the total damage sum is $D \geq 1$ a component's fail or crack is expected.

$$D = \sum \frac{n_i}{N_i} \tag{1}$$

The most important linear damage accumulation hypotheses are shown in **Figure 5** [14; 16; 17]:

Miner original:
Loads below the knee point of endurance do not contribute any damage.

$$S_a > S_{aD}\colon\ N = N_D * \left(\frac{S_a}{S_D}\right)^{-k} \tag{2}$$

Miner elementary by Palmgren:
Loads below the knee point of endurance do contribute equal damage than loads within the area of finite life fatigue strength. This method contributes to conservative designs.

$$S_a \leq\geq S_{aD}\colon\ N = N_D * \left(\frac{S_a}{S_{aD}}\right)^{-k} \tag{3}$$

Miner modified by Haibach:
Loads below the knee point of endurance contribute to reduced damage. Haibach defined the gradient of the finite life fatigue strength as $-k$ and extended the straight with $k' = -(2k-1)$ below the knee point of endurance.

$$S_a \leq S_{aD}\colon\ N = N_D * \left(\frac{S_a}{S_{aD}}\right)^{-(2k-1)}, S_a > S_{aD}\colon\ N = N_D * \left(\frac{S_a}{S_{aD}}\right)^{-k} \tag{4}$$

Miner modified by Liu-Zenner:

At load spectrum peak level Wöhler curve is rotated and further gradient is $k' = \frac{k+c}{2}$, where c is a factor for crack growth.

$$S_{aD}^{*} = \frac{S_{aD}}{2} \quad \textbf{(5)}$$

Palmgren modified by Haibach is mostly chosen for damage calculation in agricultural machines [9]. General validity of linear damage accumulation hypothesis for cyclic loads on gears has been shown by Schaller [18] for tooth flank and Suchandt [19] for tooth root.

2.2.2 Torque measurement

Torque measurement in mechanical systems such as drivetrains is mostly done with strain gauges. These offer the opportunity to measure real torque level taking all external effects such as shocks into account. Strain gauges can be applied to almost all surfaces. The measuring principle is based on the elastic deformation of materials due to forces like stretch, bend, compression and torsion stress. The strain gauge is glued to the measurement object, e.g. a shaft and changes its size similar to the measurement object. This elongation or compression varies the resistance of the metal part in the strain gauge. **Figure 7** shows a systematic draw of a metal strain gauge.

Forces should appear in the active direction of the strain gauges which maximize the change in resistance. Because these metal resistances are influenced by temperature and additional forces appearing in the shaft, a special compensation technique was developed. This so-called Wheatstone bridge, shown in **Figure 8**, uses 4 identical resistances. For torque measurement, all resistances $R_1 ... R_4$ are filled with strain gauges which are applied in 90° to each other as demonstrated in **Figure 9**. One pair of strain gauges is glued to the front side of the shaft, the other pair to the back. Because no. 1 and 4 are connected with a positive sign and no. 2 and 3 with a negative sign, this compensates external effects. The supply voltage is connected to the opposite pairs and the measurement signal is taken from the other side

of the pairs. This circuit design allows maximum stability and resistance change [20; 21].

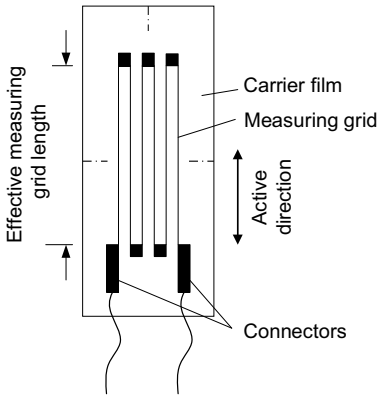

Figure 7: Standard metal strain gauge on foil carrier; [20].

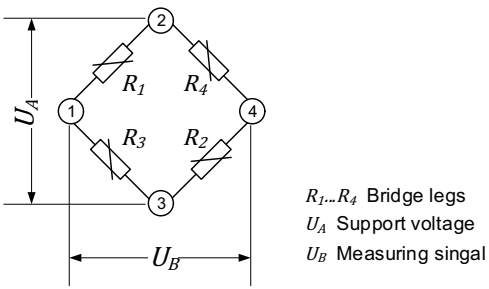

Figure 8: Wheatstone bridge; [20].

As strain gauges are passive sensors, the generated signal voltage is low and needs additional measuring amplifiers to interpret the signal. When the torque of rotating objects such as gears or shafts are to be measured, it is not possible to install a static cable connection. In such cases a telemetry system is necessary. It consists of two

antennae, one on the rotating part, the other on the static part. Supply voltage and measurement signals are transmitted wirelessly [22].

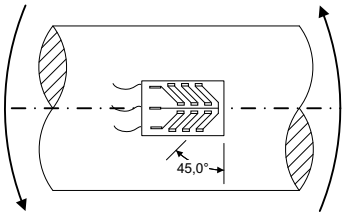

Figure 9: Strain gauge measuring set up for torsion forces on a shaft.

2.2.3 Load spectrum

Load spectra merge loads that a component or assembly was exposed during its lifetime. Radaj defines load spectra as “frequency distribution of statistically measured load amplitudes”. For standardization, load spectra are referenced as shown in **Eq.(6)** without dimensions [14]. Renius describes a load spectra as “the result of statistical analysis of a timely variable load sequence, a frequency distribution of load characteristics” [23].

$$\frac{S_a}{\bar{S}_{a_{max}}} = f(\frac{N}{\bar{N}}) \quad \textbf{(6)}$$

In practice, load spectra are generated from measured load-time-functions. Strain gauges are widely used to measure torque, but pressure or temperature can also be the relevant values for measuring component load. It is common practice that measurements with $N < 10^6$ are extrapolated to $N = 10^6$. In technical literature, a widely used form of presentation is a cumulative curve of distribution frequency with semi-logarithmic scale on the abscissa [24]. The form of these load spectra depends on a variety of factors. Basic forms are Gauß-Normal-Distribution and one-phase distribution. The most real applications result in mixed forms as shown in **Figure 10**. Radaj

names curves (2, 3) as exemplary for cranes and bridges and (5, 6) as typically for vehicles.

The curves are described by **Eq.(7)**

$$log\frac{N_i}{\overline{N}} = -6\left(\frac{S_{ai}}{\overline{S}_a}\right)^e \tag{7}$$

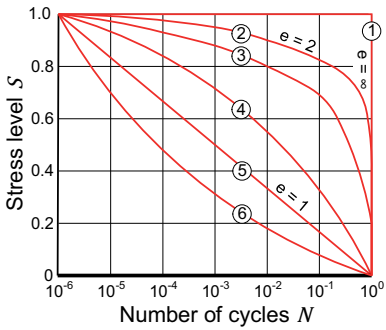

Figure 10: Different forms (distribution) of load spectra: (1) one-phase distribution; (2, 3) mixed distribution; (4) Gauß-Normal-Distribution; (5) straight-line distribution; (6) logarithmic normal-distribution; [14].

For an aggregation of the load-time function, counting methods are necessary. One-parametric and two-parametric counting methods are differentiated [14]. Two-parametric classification keeps information about load sequence and reflects the dynamic of past loads [25]. This information gets lost in one-parametric classification, which is a special case of two-parametric classification. One-parametric classification generates time-based frequencies. Speed-synchronous counting belongs to this category. Radaj lists the following one-parametric classification methods as relevant for operational stability [14]:

- *Level crossing*:
  Counting of overriding or falling below of class boundaries.
- *Peak counting*:
  Class-based counting of load peaks.
- *Range counting*:
  Counting of transitions of rising or falling loads, independent from load start level-/ load-mean.
- *Level distribution counting*:
  Counting of actual load level in constant time intervals.

The basic principles of these classification methods are shown in **Figure 11**. The choice of a method depends on the question to be solved and results in different load spectra. It is recommended to use one-parametric classification methods for drivetrain components because these deal with cyclic loads e.g. tooth flank and tooth root [25]. Several authors [12; 24; 26] propose level distribution counting for technical design of drivetrains, although DIN 3990/6 [15] requires a speed synchronous-classification. Both methods result in equal load spectra when speed is constant.

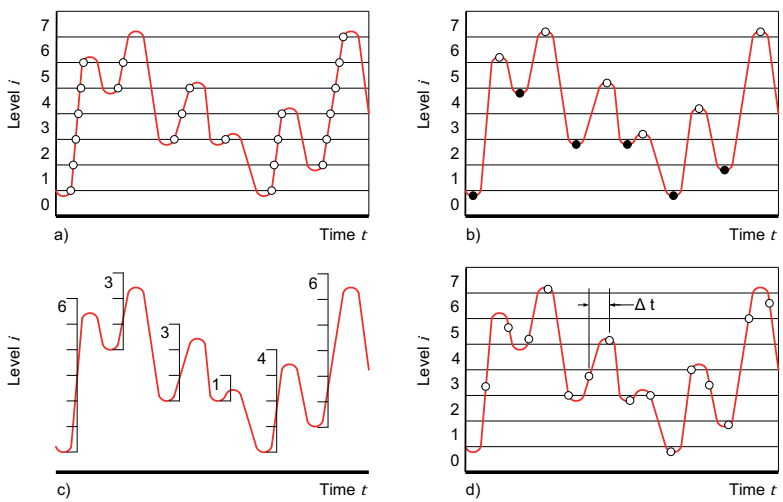

Figure 11: One-parametric classification methods: a) level crossing, b) peak counting, c) range counting, d) level distribution counting; [14].

Load spectra have been used in agricultural engineering for a relatively long time in comparison to other industries. In the 1930s, Kloth and Stroppel [27] described a method for load-recording and analysis of straw binders. Before the introduction of this method, statically-loaded components have been dimensioned by their yield point and fatigue-loaded components by their fatigue strength. The area between these technical design methods was unused and resulted in heavy and uneconomical components [14].

Renius [12] distinguishes between three load spectra for agricultural machines:

- Engine
- Drive wheel
- Driving speed

which have to represent the whole tractor life of 10,000 h. These will be explained in chapter **2.2.5**.

2.2.4 Calculation of power flow within the drivetrain

Although modern tractors have many integrated sensors, torque is rarely measured. In engines, torque is usually calculated by injection volume and actual engine revolution. Some manufacturers offer engine boost for specific operation states, e.g. speed >18 km/h or a specific power consumption via PTO [28]. This is approximated by measure of torsion in PTO drivetrain shaft [29].

Torque distribution can be approximated based on engine output torque, but this has to be corrected to compensate several losses. Pichlmaier [30] published occurring losses between engine and implement. The test tractor had a 3-axis design with two separate transmissions which caused redundancies for several auxiliaries such as steering pumps. **Table 3** gives an idea of loss distribution in tractor power flow.

Because traction effectiveness is not relevant for the approximation of torque flow the most relevant components are:

- Fan
- General transmission losses
- Air conditioner

These losses have to be considered when using torque flow approximation instead of torque measure.

Table 3: Power losses from engine to implement during grubbing (working width 6 m, working depth 20 cm), 387 kW nominal and 400 kW maximum engine power; edited from [30].

Assembly		**Component**	kW	%*
Transmission	27.5 % 44 kW	Servo pumps	5.1	1.3
		Auxiliary pump	2.1	0.5
		Lubrication pumps	1.7	0.5
		General transmis-sion. losses	35.2	8.8
Engine	6.3 % 10 kW	Water pump	4.1	1.0
		Injection pump	5.6	1.4
		Oil pump	0.3	0.1
Auxiliary units	26.3 % 42 kW	Air conditioner	6.5	1.6
		Air compressor	2.5	0.6
		Steering pumps	3.9	1.0
		Alternators	3.1	0.8
		Regulating pump	3.7	1.0
		Fan	22.1	5.5
Soil-tire contact	40.0 % 64 kW	Roll resistance	35.7	8.9
		Slip	28.6	7.1
Total power losses	**∑ 160 kW**		**160**	**40**

* percentage of losses based on P_{max} = 400 kW

2.2.5 Application load spectra

2.2.5.1 Engine and gearbox input

Engine operation behavior can mainly be described by a matrix of speed and engine load which equals output torque. The percentage of idle time, which is engine at idle speed at low engine load, is important when evaluating tractor operation hours. John Deere assumes average engine idle time in tractors of 25 % [1]. Engine load spectra are highly related to gearbox input load spectra and are described in the following.

In 1956, Gerlach published a load spectrum for heavy ploughing of the *gearbox input* side which equals engine output without auxiliaries, **Figure 12**. Classification was done as a histogram of 10 classes and measured clutch torque was standardized on engine nominal torque as shown in **Eq.(8)**. The median of the measure was 76 % [31].

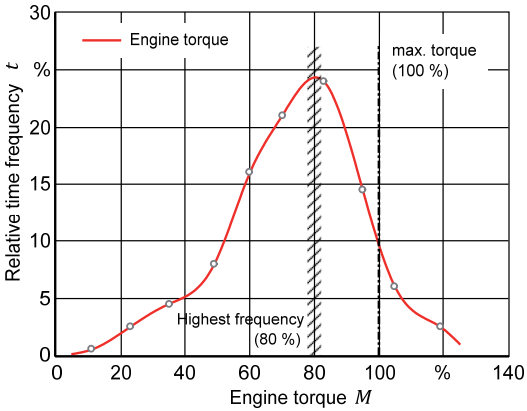

Figure 12: Load spectrum of gearbox input torque during heavy ploughing application (without idle, start/stop and switching operation); 22 kW standard tractor, rear drive, level distribution counting; from [31].

$$M = \frac{Torque_{Clutch}}{Nominal\ torque_{Engine}} \quad \textbf{(8)}$$

The holistic load spectrum of agricultural work of a tractor was described by Coenenberg in 1963 [32]. Similar to Gerlach, Coenenberg did not take stop-and-go and switching operation into account. Because PTO torque was not measured, the median was at 35 % which is shown in **Figure 13**. The author assumes 80 % average engine speed which relates to 28 % drivetrain power.

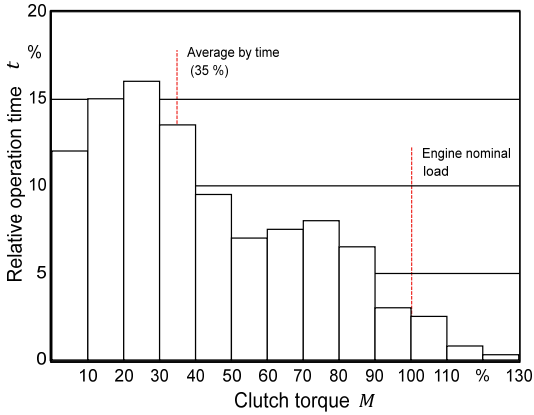

Figure 13: Load spectrum of gearbox input torque during tractor lifetime (10,000 h) (without start/stop and switching operation); 22 kW standard tractor, rear drive, level distribution counting; from [32].

Another study from Coenenberg describes the absolute frequency of torque peaks at gearbox input shaft. While level distribution classification leads to standardized torque levels of 100 % to 130 %, torque can reach peaks up to 300 % of nominal engine torque [33].

In 1976, Renius published an approach for standardized load spectra on the basis of level distribution classification. In addition to the results of Coenenberg and Gerlach the standardized load spectrum covers all operating states and 95 % of all agricultural tractor applications [12; 9]. An automatic load limit control was not considered. The curve in **Figure 14** is based on:

I. Total lifetime of 10,000 h, equals 0 % of engine nominal torque and 100 % relative frequency
II. Average engine torque by median of time, equals 40 % - 45 % of engine power and relates to 56 % of engine nominal torque for 80 % average engine speed, relative frequency 50 %
III. Maximum engine torque, highest static load for gearbox input shaft, 108 % - 115 % of engine nominal torque, equals 4,5 % relative frequency

IV. Dynamic torque peaks, mainly caused by switching operation or clutch slipping once per 25 h (accumulates to 0,033 h time) reaches over 250 % of engine nominal torque.

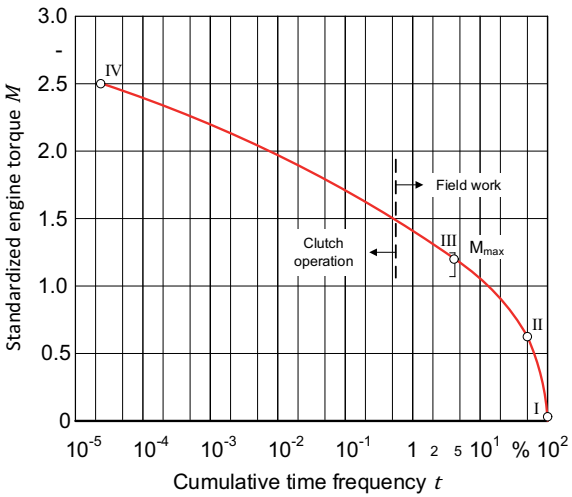

Figure 14: Load spectrum of gearbox input torque during tractor lifetime (10,000 h), slightly hard conditions, 30 - 110 kW standard tractor, rear drive, level distribution counting; [12].

While the curve up to 150 % nominal engine torque is dominated by applications, the area in between 150 % and 250 % is defined by shifting operation in correlation to the type of transmission. Powershift transmissions have a higher amount of torque peaks than manual shift transmissions, due to their functional principle [12]. Modern continuous variable transmissions (CVT) do have less peaks because of fewer or no shifting operations compared to powershift or manual shift transmissions.

2.2.5.2 Gearbox output

Gearbox output load spectra are influenced by a variety of parameters. Renius [12] identified

- Empty machine weight
- Radius of the largest drive wheel
- Gross vehicle weight

as the most important factors, because of their direct influence on torque levels in the drivetrain. A standardized load spectrum for the driving wheel side can either be based on **Eq.(9)** or **Eq.(10)**.

$$M = \frac{Torque_{Drive\ wheel}}{G_{net} * r} \quad \textbf{(9)}$$

$$M = \frac{Torque_{Drive\ wheel}}{\frac{G_{net} + G_{max}}{2} * r} \quad \textbf{(10)}$$

Although Eq.(10) takes greater account of reality, gross vehicle weight is only a regulation. Eq.(9) uses machine empty weight, a real and comparable weight for standardization of torques. When machine gross weight equals 1.7 - times machine empty weight both standardization approaches have the same scale. An analysis of 250 currently available standard tractors showed an average ratio of 1.67 with standard deviation of 0.19. **Figure 15** shows a comprehensive load spectrum for a standard tractor with rear wheel drive. The spectrum covers 95 % of all applications but does not take very heavy and specific applications such as soil loosener into account [9].

Although the author publishes a load spectrum for the driving wheels, it is listed under gearbox output because the sum of a standard rear-wheel driven tractor equals gearbox output, corrected for differential and final drive ratio.

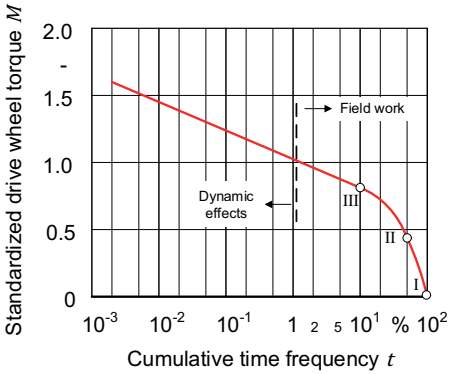

Figure 15: Load spectrum of drive wheel torque during tractor lifetime (10,000 h), slightly hard conditions, 30 - 110 kW standard tractor, rear drive, level distribution counting; [12].

The drive wheel load spectrum is defined as follows:

I. Total lifetime of 10,000 h, equals 0 % of engine nominal torque and 100 % relative frequency

II. Average drive wheel torque of 45 %, 50 % of the time

III. Heavy pull applications like ploughing are calculated by average traction coefficient μ and represent the maximum pulling force in standard conditions. μ, ρ, κ for different soil types and conditions were published by Steinkampf [34].

At 1 % time frequency the maximum traction force of a heavy-ballasted tractor is reached. This is the upper end of operational loads. Drive wheel torque above 1.0 is caused by dynamic effects during field work.

Biller published a load spectrum for the left driving wheel shaft of a 70 kW tractor. Three applications were recorded and displayed in **Figure 16**. Data are standardized by the Renius equation Eq.(9). Negative loads do not exceed 45 % of the positive loads and their cumulative frequency stays below 10 %. A variation of the application mix influenced the overall load spectra only partially in moderate height [24].

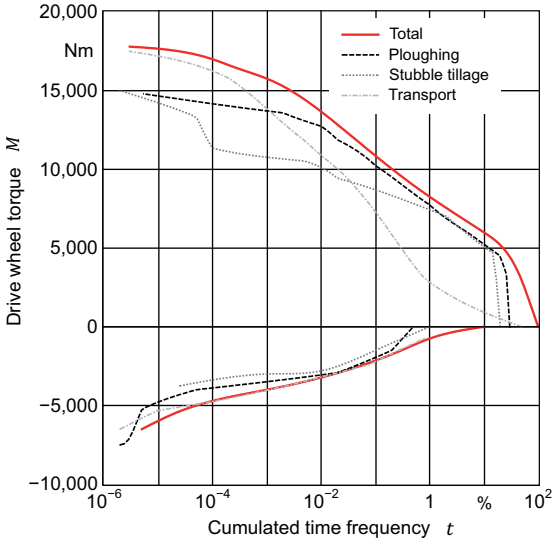

Figure 16: Load spectra of different applications including negative loads. The overall load spectra is divided into 29.83 % ploughing, 21.39 % stubble working and 48.78 % transport; adopted from [24].

2.2.5.3 Axles

Kühlborn published load spectra of driving wheels of conventional ploughing. In the first experiment the standard tractor used rear drive only. Contrary to expectations, the median of the load distribution was not similar between the left and right side [35]. The deviation of the left and right driving wheel are discussed by Renius [12] and displayed in **Figure 17**.

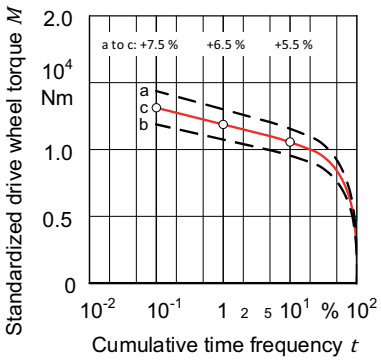

Figure 17: Load spectrum of driving wheel torque during ploughing, medium conditions, 70 kW standard tractor, deactivated front wheel drive, level crossing counting. a = right wheel (in the furrow), b = left wheel (on land), c = average of a and b (equals 50 % of load spectrum for driving wheels); [12].

The deviation between minimum and maximum are 5.5 % and 7.5 % and are caused by friction in the axle differential. Later trials show average deviation of 10 % to 15 %. These effects annul themselves by time so that Renius tends to add 5 % on top of the half driving wheel load spectrum in case of non-lockable differentials. For lockable differentials Renius recommends 8-10 %.

Today, MFWD tractors are state of the art. A later load spectra, based on the original one from 1976, distinguishes between total load and rear axle load [9]. Renius recommends a factor of 0.8 for standard tractors and a factor of 0.75 for large tractors. For MFWD-system tractors, which are characterized by 4 equal-sized wheels, and very large standard tractors, the factor can be reduced to 0.7.

Meiners mentions two important applications for front axle loads:

- Field work with engaged front wheel assist
- Front loading

Total activation time of the front wheel assist is estimated 30 - 60 %. Ratio of field work and front loading in **Figure 18** is 10:1 [36].

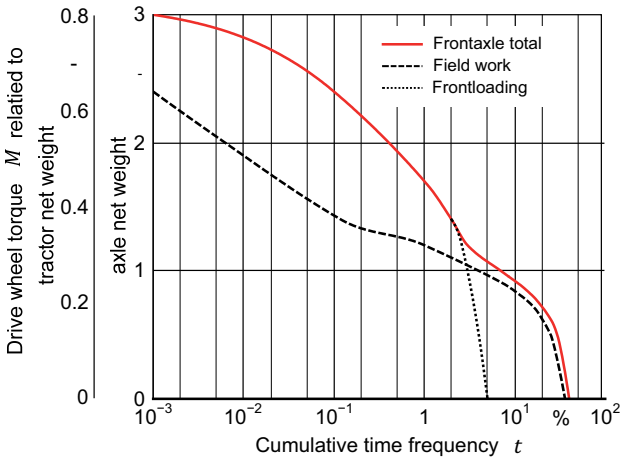

Figure 18: Load spectrum of tractor front axle for different applications, torque standardization by tractor net weight or tractor front axle weight; from [36].

2.2.5.4 PTO

Modern tractors are equipped with front and rear power take-off (PTO). It transfers engine power to an implement in the back or front of the tractor. Depending on the application spectrum and tractor class, usage of PTO varies over a wide range. PTO load spectrum depends on type of application. Biller [37] measured 1983 PTO loads for rotary harrow, harrow and a rotovator, **Figure 19**. The cumulative frequency is based on 100 % PTO on time. The overall load spectrum is calculated by weighing harrow 6 %, rotary harrow 34 % and rotovator 60 %. Either speed or working depth were varied within one application.

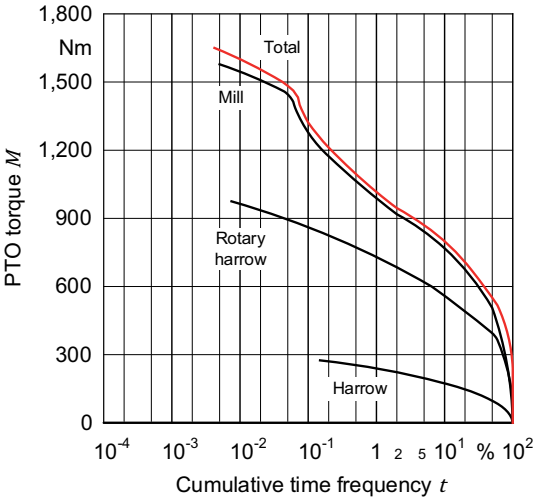

Figure 19: Load spectra for PTO applications and overall PTO load spectra; [37]

Meiners recorded detailed PTO load spectrum for different applications [36]. He distinguished between heavy und light PTO applications and calculated an overall load spectrum for both which is shown in **Figure 20**. Measured torque is standardized to nominal PTO torque, which in stationary condition and smooth loads, equals enqine output torque. Dynamic peak effects as they appear during baling superelevate to twice nominal PTO torque. Cumulative frequency does not reach 100 % time because data refers to total tractor operation hours. This seems quite high compared to current fleet analysis. The German Agricultural Society (DLG) powermix test distinguishes between rotary harrow, mowing, manure spreading and baling for PTO application [38]. Load intensity is varied within an application.

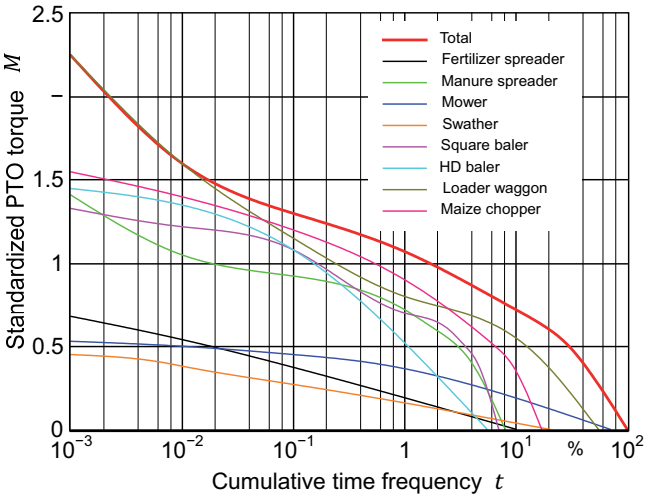

Figure 20: Overall and application specific PTO load spectra for different heavy PTO applications; from [36].

With the exception of singular contractors, most tractors use the PTO at a low level of time and medium intensity. Without a separate torque sensor in the PTO drivetrain actual loads are hard to determine. In the case of a parking tractor, all consumed power is transferred to the PTO, so PTO torque equals engine output torque. But in the case of a driving or pulling tractor, engine output torque is split variably between driving wheel and PTO. It is not possible to determine this split ratio without having torque sensor on PTO side which is not common for most of the tractors. For this reason, the PTO is not the focus of this research.

2.3 Approaches machine health index

2.3.1 Definition of maintenance concepts

Maintenance plays a considerable role in the lifecycle cost of a product. Until recent years, maintenance-free or reactive maintenance strategies were considered-state-of the art. **Figure 21** displays different maintenance methods and how they handle failure. For some applications like bearings which cannot be easily accessed, maintenance-free design is required, but costs are disproportionately high [3; 39].

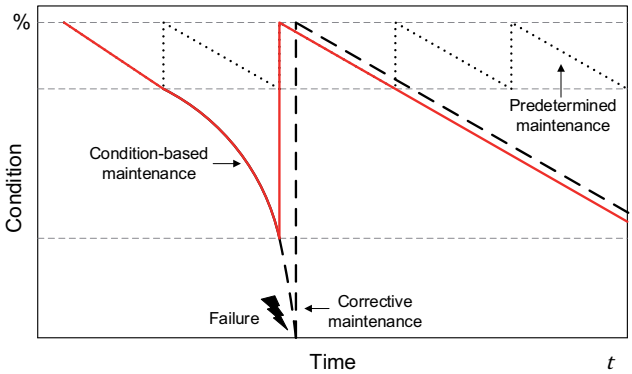

Figure 21: Maintenance principles: predetermined, corrective and condition based maintenance; edited from [40].

Reactive maintenance provides maintenance only after a failure occurs, so called “fire brigade strategy”. This maximizes usage of a component’s capacity and simultaneously reduces cost. But it does not take the cost for a machine’s downtime into consideration which might be much higher compared to a proactive maintenance strategy. Sometimes broken components cause further damage to the system or increase the risk of hazards [3]. A worn bearing of a water pump in a combustion engine can induce slip on the synchronous belt which controls valve opening and closing. In the worst case, valves and up-moving cylinders can come into contact, bend and will cause total engine failure.

Preventive maintenance is now state-of-the-art for a wide range of machines and applications, demanding high operational-safety or prevention of secondary induced damage. To achieve that components are replaced by operation hours, time in general or other parameters such as distance travelled and amount of fuel consumed. As loads vary over a wide range, maintenance intervals have to guarantee uptime under all circumstances. In some cases a component will be worn out just before the regular service but most times a certain amount of remaining lifetime is not used. This maintenance strategy is characterized by high uptime rates and high maintenance cost. Under the heterogeneous circumstances in agriculture the gap between high-loaded and low-loaded machines, which all have to be covered by one maintenance interval, is even bigger. This has a negative influence on a product's lifecycle costs. A well-known example is the changig of a combustion engine's oil on the basis of operation hours. Depending on the manufacturer, common intervals are 500 hours independent from actual usage characteristics [3; 41; 42].

Condition based maintenance (CM) means maintenance only on demand. As shown in Figure 21, a failure can be detected by condition monitoring before it actually appears and can be fixed before the component is broken. Wear-related parameters are monitored and compared with defined limits and thresholds. When a parameter breaches the set threshold, maintenance will be initiated. Modern cars, for example, detect wear on disc brakes. Replacement of brake pads is done conditionally. This increases machine uptime, maximizes the usage of components' reserves and reduces maintenance costs [43; 44].

The *predictive maintenance* (PM) concept is defined as "comparison of measured physical trends against known engineering limits for the purpose of detecting, analyzing, and correcting problems before failure occurs" [45]. This strategy is based on additional wear-related sensor data - typically temperature, rpms, oil quality, acoustics or vibrations. Using one or a combination of several parameters enables identification of partial degradation or wear of components, far before the occurrence of a functional error in the system. At this time maintenance can be done cost efficient and "domino" damage is avoided. Sensors and analysis technology are the subject of today's research [46; 47]. Most systems work by measurement of shifts in zero point or trend analysis [48]. By analysis of degradation trends, an estimation for the remaining lifetime and the optimal point of maintenance is calculated [3].

While condition monitoring needs additional sensors to measure wear-related parameters, *load cycle monitoring* is a different approach. Based on the knowledge of wear and damage mechanisms, relevant parameters are measured permanently during machine operation. These parameters are classified and compared to a given reference. In truck-mounted cranes, a load cycle monitoring system records actual loads on the crane's winch and calculates remaining load cycles. Although the approach considers actual loads, individual non-standard influences like manufacturing defects are not detected. The load cycle approach is somehow related to "out-of spec" monitoring, shown in **Figure 22**. It registers the time that a system or component, for example a hydraulic pump, is operated over a certain pressure, temperature or flow. In combination with the knowledge of wear mechanisms, out of spec monitoring gives an indication of a system's or machine's condition [3].

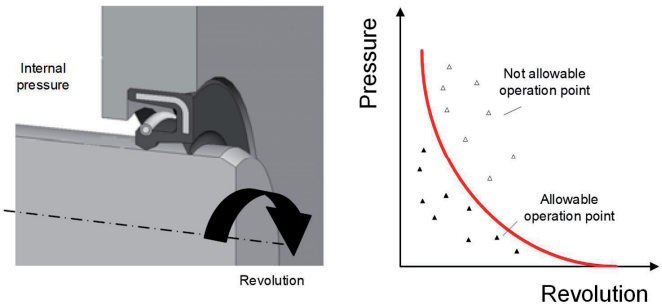

Figure 22: Classification of inner pressure and revolution of a rotary shaft sealing into allowable and not allowable operation points; edited from [3].

Although science has established clear definitions for maintenance approaches, in practice, terms are not always used precisely. CM, PM and load cycle monitoring are mixed frequently and especially industrial manufacturers use the different approaches in combination. The following section lists examples for CM, defined in 2.3.1.

2.3.2 Examples of condition monitoring

Many researchers concentrate their studies on the field of condition monitoring. Wind turbines and tooling machines are in the focus of these reviews [49]. **Figure 23** shows an enormous increase in publications for CM in wind turbines. The main reasons are the harsh environment, poor accessibility of most wind-generated power plants, in particular the offshore ones and those with high varying loads [50]. The following introduces some approaches of condition monitoring in power, industrial and mobile applications.

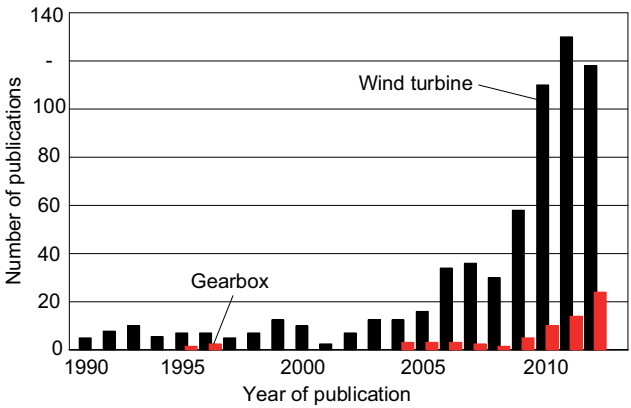

Figure 23: Publications in the field of condition monitoring in wind turbines: Total number of publications and specific ones for gearboxes; from [49].

The application of condition monitoring in *tooling machines* has been comprehensively reviewed by Botsaris and Tsanakas [51]. Besides the discussion of hard and soft faults, the authors review monitoring methods, signal processing techniques, classification and diagnostic tools. Tool condition is influenced by two types of faults. **Figure 24** presents the progressive development of soft faults which result in gradual degradation of tools. This type of wear is predictable. Consequently, hard faults are unpredictable. There is consensus that analytical models and numerical methods have a disadvantage in accuracy compared to CM methods.

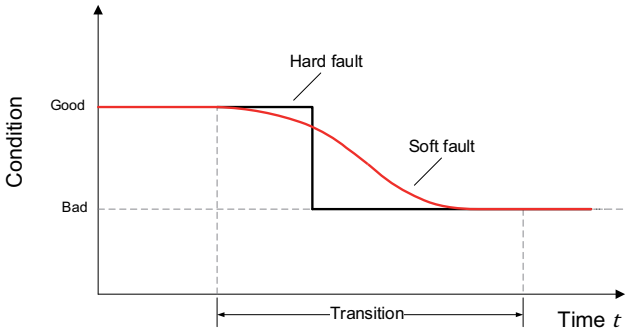

Figure 24: Principle of hard and soft failures; from [51].

While tooling machines have relatively constant loads or rotation states at some point in the process, *industrial robots* do not. Velocities of joint and path change during the sequence result in high acceleration and deceleration phases. There is almost no period of constant speed. Consequently, static loads depend on the spatial position and dynamic loads on acceleration and geometrical position. Possible solutions are either measuring vibration spectra at different times to detect deviations, or establishing an unloaded test cycle, to reduce variance in parameters [52].

According to Tchakoua et al. [50] it is failures of *wind turbine's* gearboxes which are responsible for most of their downtime. The basic idea behind the widely used vibration analysis approach is that rotating machines have specific, condition dependent vibration signatures.

The vibration spectra changes with ongoing degradation thus measuring wear and damage can be performed by trend analysis [47; 40]. Because some teeth lose their stiffness or even breach, as shown in **Figure 25**, peaks in acceleration appear with each revolution and mark the damaged teeth. Most of the CM techniques are standardized in ISO10816-3 [53]. In addition to vibration analysis, other common methods are oil-debris analysis and temperature measurement. Techniques from structural CM, which are described later, as well as human inspections, are also in the monitoring portfolio [50; 40]. Nevertheless, varying loads and changing environmental conditions

such as temperature and humidity, affect this approach in a negative way and increase the probability of false-negative predictions.

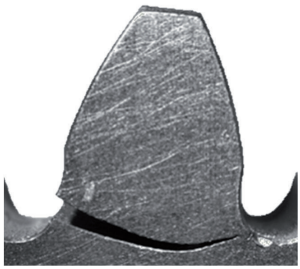

Figure 25: Fatigue crack in a gear‘s tooth root; [54].

Since the mining industry has replaced haul trucks with large conveyors, condition monitoring has become interesting in particular. These conveyors are typically single points of failure and have high criticalities. Recent studies indicate that up to 90 % of malfunctions are predictable. A condition monitoring system has the advantage of failure prediction while most automation systems only monitor sensor data. Conveyors generate vibration signatures, which are certain and predictable, and correlate with wear and load. Temperatures can also be monitored, but only in controlled environments like buildings where ambient conditions have less impact on measured temperatures. Conveyors in open-pit mines can replace haul trucks, but are the bottleneck of the whole mining business, thus reliability and uptime must be granted by continuous CM of the conveyor [55].

A large original equipment manufacturer (OEM) for construction and mining machines, has installed a remote condition-monitoring system. It analyzes different data elements which are shown in **Table 4** such as electronic data, fluid analysis, inspection data, repair history and site conditions. Processing is performed off-site combined with expert knowledge of the equipment. Benchmarking of the individual machine to a standard, a local fleet or a global fleet of machines can be performed additionally [44].

Table 4: Data groups and data sources of a remote condition monitoring system for minig machinery; edited from [44].

Data group	Source
Electronic data	On board electronic data
	OEM
	3rd party
Fluid analysis	Engine
	Transmission
	Torque converter
	Axle compartments
	Hydraulic systems
Equipment inspection	Checklist
	Findings
Repair history	Work order history
	As built information
	Machine specification data
	Component life data
	Maintenance schedules
Site conditions	Haul road profiles
	Weather
	Temperatures, elevations

With the accident of a German ICE 1 *train* in Eschede on 3rd of June 1998, the risks of fatigue received high attention in the rail sector. A broken wheel ring caused the train to derail and hit a bridge, injuring 88 and killing 101 people [56; 14]. Since the classic monoblock wheel design caused noise and vibration at operational speed, the engineers decided to add a 20 mm rubber ring to separate wheel rim and central disc wheel body. This led to unexpected high loads on the rims. These were imperceptibly flattened into an ellipsis with each revolution (500,000 per day), and resulted in fatigue [57]. Since that day a lot of research on CM in trains and tracks has been done. Ho et al. [58] assessed both - monitoring systems on the train and on the rails. Because of electromagnetic interferences which are normal on trains, the authors used optical sensors for measures. Breaches in the rail and non-round wheels could be detected by differences in wheel vibrations.

Tsunashima et al. [59] detected track irregularities by measurement of vertical and lateral acceleration. By using an additional gyroscope, the researchers were able to

distinguish between line irregularities and level abnormalities. Corrugation was sensed by noise via spectral peak calculation.

2.3.3 Comprehensive condensation of vehicle operation data

2.3.3.1 Health index/load factor

Interpretation of load spectrum data is complicated and requires expert knowledge. For this reason, the objective of a single number representing the holistic machine condition emerged. This so-called health index is defined in ISO 13374-1. A suitable range for the value of a health index should be between 0 and 10 [60].

Klanfar defines the engine load factor as a percentage of the rated engine power that is utilized during work process [61]. The calculated factors range from below 0.1 during idle and 1.0 during full load operation. Ryken und L'Heureux calculate an average engine load factor on a time weighted basis [62]. However the load factor shows utilization of an assembly, for example engine, gearbox or axles by means of relating it to a defined reference.

2.3.3.2 Examples of condensation of values

Carfax, an American company, offers *vehicle history reports*. Potential customers of used cars can gather information about former owners, accidents and other reported damages such as flooding or frame bending, OEM recalls and service records [63]. With this information, customers get a detailed look at a car's history and can decide whether to buy it or not. The idea is closely related to Akerlof's publication "The market for lemons" [10] which describes the automobile market in the US. Assuming there are only four kinds of cars: new ones and old ones, good ones and bad ones, which are called "lemons", Akerlof predicts that used cars tend to be lemons because otherwise they wouldn't be for sale. An asymmetry in information between the owner, who can form a good idea about quality of the vehicle, and the potential buyer, is the reason for this phenomenon. Carfax balances this asymmetry by providing more information to buyers.

Mercedes Benz' telemetry system called FleetBoard is a management tool for truck fleets. It mainly consists of three modules: vehicle, logistic and time management. Analysis of *driving behavior* and *task difficulty* are two services included in FleetBoard. The analysis is done based on a variety of parameters which are listed in **Table 5**. Final results are graded from 1 = poor, up to 10 = very good. While these parameters are condensed in two "scores", other parameters such as driving time, idling time, percentage of operational brake, percentage of wear-free brake, distance in overrun or percentage of high speeds are monitored. An automatic analysis or further condensation is not done. Users have to interpret these numbers by themselves. [64]

Table 5: Considered factors for driving behavior and task difficulty evaluation for on road trucks; from [64].

Score	Parameter	Factor
Driving behavior	Anticipatory driving	Fuel consumption
		Brake usage
	Engine characteristic driving	Switching behavior (transmission)
	Accelerator pedal	Continuous usage
		Number of changes in pedal position
	Constant speed	Number of changes in speed
	Stops	Number of stops
	Deceleration/ braking	Brake pedal position
		Number of emergency braking
Task difficulty	Slope coefficient	Ascend
	Stops	Number of stops
	Weight	Total transportation weight

Patent DE 3104174A1, approved in 1981, describes a method which takes into account real engine load to calculate *maintenance intervals* for passenger cars. The inventors criticize static distance-based maintenance. Distance-related triggers have to take all environmental factors into consideration, resulting much earlier than necessary in a repair or replacement of parts. Total fuel consumption is, contrary to distance, a parameter which positively correlates with load and wear. Under extreme conditions such as cold start, high speed drive or stop and go, fuel rates are higher than under

optimal conditions. Total fuel consumption is an appropriate measure for total engine wear. [65]

DE 102006046157A1 describes a procedure for operation of large diesel engines. The approach uses operation data which are generated and protocoled by an engine control unit (ECU). On this basis, *variable maintenance intervals* are generated. While passenger cars calculate one interval for the whole engine, the system provides individual intervals for specific assemblies. This takes load-dependent wear into account. The approach classifies different engine loads and provides a weight factor for each class, which is recognizable from **Table 6**. By multiplying these by the specific operation time in this class, a load based-maintenance interval can be calculated [66]. Because wear factors are companies' classified expert knowledge Table 6 only shows fictitious numbers.

Table 6: Procedure for calculation of individual maintenance intervals in large diesel engines by weighting of operation points; [66].

Engine load (EL)	Weight factor (WF)	Real operation hours (ROH)	Calculation ROH * (1 + WF)	Virtual operation hours (VOH)
%		h		h
101 - 110	+ 0.25	5,000	5,000 * (1 + 0,25)	6,250
76 - 100	0	5,000	5,000 * (1 + 0)	5,000
31 - 75	- 0.25	5,000	5,000 * (1 - 0.25)	3,750
11 - 30	- 0.40	5,000	5,000 * (1 - 0.40)	3,000
0 - 11	- 0.50	5,000	5,000 * (1 - 0.50)	2,500

DE 10349875A1 relates to calculation of a *wear index of combustion engines* [67] by a comparison of two or more parameters. An approach for the wear of engine's tooth belts is given in DE 19944435A1. Mathematical transfer functions have been developed from bench tests an wear can be estimated from actual operational data [68]. DE 10029634A1 describes a comprehensive procedure to calculate maintenance requirement by measuring of parameter's deviation from reference values [69].

DE 102015214357A1 describes a system and procedure for *estimation of remaining lifetime* (ERL) of components in a drivetrain. It uses gearbox sensor information like torque and RPM to calculate damage. The ERL processing is not further specified [70].

Telemetry systems are state of the art in a wide variety of branches [64; 44; 71; 72]. Mobile off-highway machines such as construction machines [44], snow groomers [73] or agricultural machinery [74; 62; 75; 76] use this wireless data transmission technique.

An onboard modem collects data from different control units from the controller area network (CAN) bus and transmits the data via cellular networks to servers. These systems are mainly used for real time fleet surveillance, yield tracking, timekeeping, task management, geofencing, benchmarking of machines and maintenance reporting. Behind customer's features, OEMs can mine stored data as the example from John Deere's 2011 established JDLink™ shows [62]. Tractors are categorized by duty cycle using accumulated engine hours and engine load factor (cf. 2.3.3.1). Further parameters are region and time period. Percentiles have been calculated for the sum of engine hours and average engine load for each tractor. By defining upper and lower percentile, tractors are split into 4 different categories, listed in **Table 7**. High-usage tractors make up 0.6 % of the population, low-usage tractors 2 %. Ryken und L'Heureux make further comparisons of customer tractors and company's test tractors to compare engine load distribution.

Table 7: Categories for standard tractors based on customer duty cycle; [62].

		Engine load factor		
		Low	**Average**	**High**
Engine hours	**High**	High hour tractors		High use tractors
	Average			High load tractors
	Low	Low use tractors		

Because agricultural machinery and especially tractors have a wide range of applications, machine features are used to different extents. Evaluation of feature usage on time basis between the population and high hour tractors was performed. The features

analyzed were: engagement of automatic guidance, mechanical front wheel drive, differential lock, rear power take-off and transmission mode.

The telemetry system of OEM CLAAS, called Telematics, launched in 2005, has similar functionalities. About 60 attributes are logged with sample rates depending on machine category from 0.1 Hz to 0.066 Hz [77]. Campaign reports for individual machines as well as for the entire fleet can be generated. Collected machine data are split into average, maximum and sum of all machines per attribute.

A *remote vehicle health monitoring system* was established by KOMATSU in 2002 for large-sized construction machines. While the company uses statistical processing for troubleshooting on smaller machines, the number of large machines is smaller so that individual machine diagnosis is required. A wide part of data processing is done automatically, but some still has to be evaluated manually. Indicators for machine health are:

- Machine usage spectrum
- Rigorousness of operating condition
- Estimated remaining lifetime

Besides onboard CAN-bus data monitoring, periodical inspections, oil analysis and failure recording is taken into account. The authors refer to over 70 machines equipped with a vehicle health monitoring system, requiring less maintenance, which results in less unplanned downtime. [78]

Table 6 gives a good idea about the problematic of scientific work on the field of load evaluation. OEMs present purchasable solutions and own patents but do not share their knowledge about specific wear mechanisms and damage evaluation procedures.

3 MATERIAL AND METHOD

3.1 Overview

An overview of the method is shown in **Figure 26**. The procedure can be divided into 4 main steps which are briefly described as follows:

Measurement, 3.2:
Data recording for each assembly and different applications during field tests. Basis for generation of load spectra.

Scenario, 3.3:
Definition of 5 different application scenarios for tractor lifetime. Calculation of tractor lifetime load spectrum for each assembly.

Load calculation, 3.4:
Calculation of assemblies' individual load sums based on pseudo damage calculation. Introduction of assembly specific reference load spectra level. Calculation of reference load sums.

Load factor 3.5.1:
Calculation of assemblies' load factors. Evaluation of assembly specific stress in comparison to the reference. Consolidation of individual load factors to a tractor encompassing load factor. Adjustment of tractor operation hours to standard operation hours based on load factor.

Comparison 3.5.2:
Comparison of different tractors on assembly level to identify assembly-specific advantages or disadvantages in terms of past load. Comparison of encompassing load sums. An evaluation of overall tractor stress can be made.

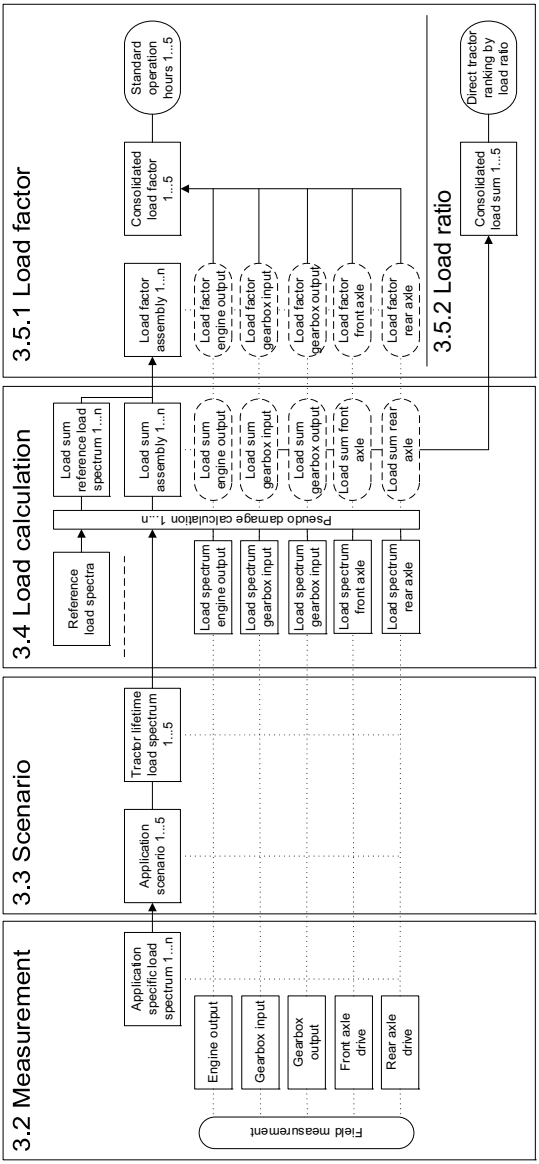

Figure 26: Overview of methodic procedure, detailed explanation in the following chapters.

3.2 Measurement and load spectra

An overview of the methodic steps for chapter 3.2 is given in **Figure 27**.

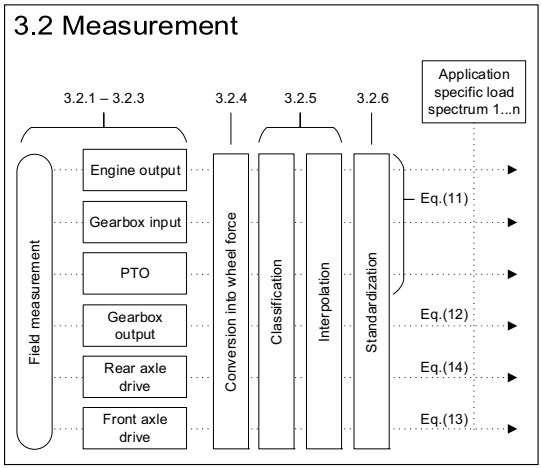

Figure 27: Detailed view of methodic part measurement: from field measurements to application load spectrum.

3.2.1 Measured applications

Data of tractor field operation was recorded during a CLAAS internal project which covered the years from 2013 to 2015. The measurements were done for different applications. Number of cycles indicates number of repetitions during the measurement:

- Heavy pull
  Grubbing and ploughing, front wheel assist, 8.1 h, 168 cycles, average field length 250 m
- Transport
  Soil and slurry transport, front wheel assist only during breaking, 57.7 h, 109 cycles, 6.8 km
- Manure/slurry
  Disc spreader and slurry tank trailer, front wheel assist, rear PTO 1,000 min^{-1}

and 540 min^{-1}, 25 h, 81 cycles, average field length 275 m, average road travel 5.8 km

- Greenline
  Mowing of grassland, front wheel assist, front PTO, rear PTO 1,000 min^{-1}, 9.4 h, 396 cycles, average field length 240 m
- Baling
  Square baler, straw harvest, no front wheel assist, rear PTO 1,000 min^{-1}, 10.3 h, 376 cycles, average field length 375 m
- Silage
  Compaction of corn silage, 9.7 h, front wheel assist, 70 m long silage pit
- PTO
  Corn grinding, stationary application, rear PTO 1,000 min^{-1}, 7 h

3.2.2 Measuring set-up: Test tractor

A MFWD tractor (135 kW; ECE R 120) with CVT was used for measurements. **Figure 28** displays the layout of the drivetrain and measuring points. Torque measurement was done with calibrated metal strain gauges. This measurement principle is described in chapter **2.2.2**. The strain gauges were glued as full bridge in a Wheatstone circuit. An angle of 45° to the central axis of the shaft was chosen to achieve maximum signal output of the strain gauges.

A telemetry system was used to exchange data from strain gauges on the rotating shafts to the measurement amplifier. Sample rate during the field tests was 1 Hz. Data was stored on the data logger and has been transferred to a database. The measurements have been georeferenced via global positioning system (GPS). Data recording and processing was done with National Instrument's software DIAdem 2015. An exemplary measurement is shown in **Figure 29**.

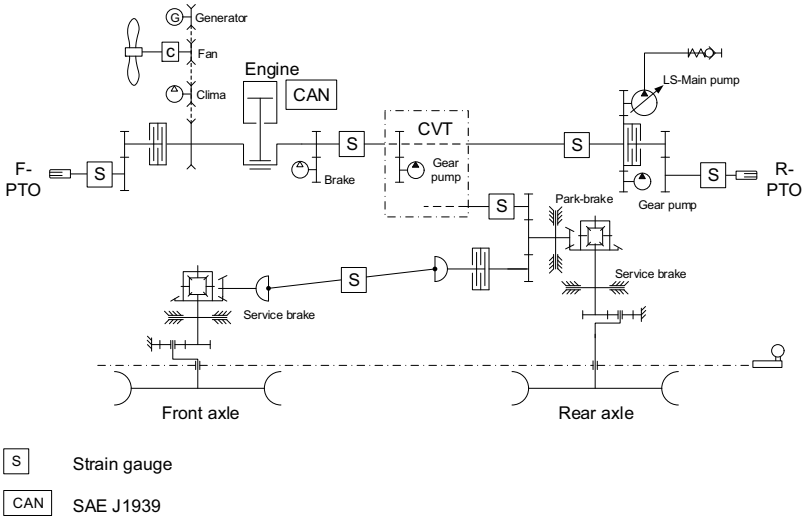

Figure 28: Functional scheme of the test tractor drivetrain and measuring points; [79].

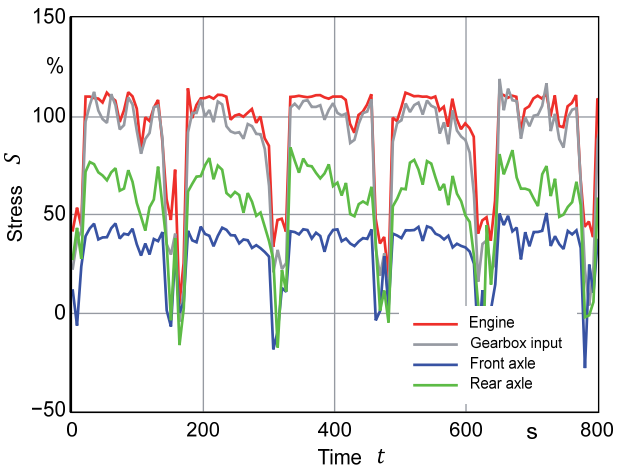

Figure 29: Raw data from strain gauge measurement of different tractor assemblies during a heavy pull field application.

In **Figure 30** a working time scheme from Reith et al. [80] is shown which is based on the “Kuratorium für Technik und Bau in der Landwirtschaft” working time scheme [81]. The analysis of the measured data was done for execution time *t11* and turning time *t12* which equals productive time *t1*. Fault time *t2* and non-productive time *t3* were not considered. Consequently, the resulting data show higher load density than during real tractor life, since idle times with low loads come on top in addition later.

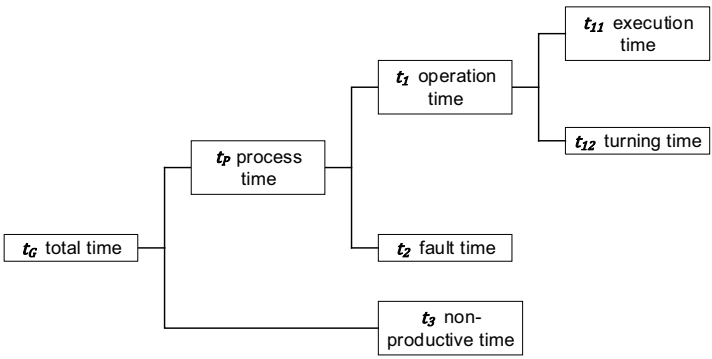

Figure 30: Working time scheme in extracts; from [80].

3.2.3 Sample rate

A sampling factor equal to 10 is widely used for measurements in practise. This means the sampling rate has to be 10 times higher than the maximum frequency expected in the spectrum. Thus, errors made at high frequencies are lower than 5 %. Lalanne demands sampling factors between 16 and 23 to reduce errors to 2 % or even 1 % [82].

The effect of different sampling rates of the attribute engine speed over a time period of 60 seconds is shown in **Figure 31**. While the raw data was logged with 10 Hz, virtual logging has been done with 5, 1, 0.5 and 0.1 Hz. Linear interpolation was performed. It is clearly visible that the 5 Hz curve follows the 10 Hz closely, minimal error occurs

at 1 Hz, increasing at 0.5 Hz and 0.1 Hz. At 0.1 Hz the curve smooths out all maximum and minimum events in between the 10 second sample points.

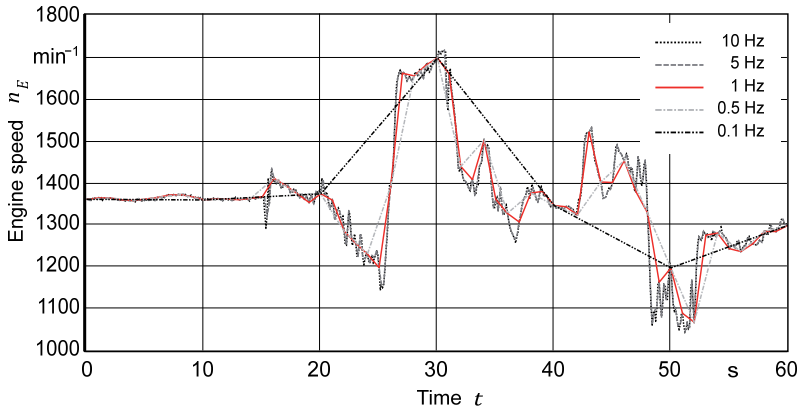

Figure 31: Different sample rates (10, 5, 1, 0.5 and 0.1 Hz) for tractor engine speed during grubbing.

Sample rates of 1 Hz are widely used during long term field test measurement. 0.1 Hz is used for remote applications such as telemetry systems. To assess the effect of sample rate under real operation conditions, classification of 3 tasks - grubbing, square baling and maize transport - was analyzed. The parameters were engine speed in 8 classes and engine load in 10 classes. The test tractor is described in chapter **3.2.2**.

Table 8 lists deviation of engine load, calculated with reduced sample rates, compared to classification of raw data at 10 Hz. Error value increases with lower sampling rates, but stays below 0.5 %, except the variant 0.1 Hz which shows a deviation up to ±2.69 %. All calculated total engine loads are close to reference at 10 Hz and show low variance.

Table 8: Deviation from reference engine load (10 Hz) during different tasks and 5 lower sample rates.

Task	Sample rate				
	10 Hz	**5 Hz**	**1 Hz**	**0.5 Hz**	**0.1 Hz**
Grubbing + Displacement (1:45 h)					
Engine Load %	46.13	46.16	46.18	46.21	45.38
Error %		0.06	0.08	0.09	2.69
Maize Transport (3:12 h)					
Engine Load %	44.13	44.14	44.09	44.00	44.23
Error %		0.00	0.04	0.23	0.09
Square Baling (3:42 h)					
Engine Load %	60.83	60.83	60.86	60.82	60.69
Error %		0.01	0.04	0.03	0.18

Table 9: Average errors per class, dependent on different sample rates; for grubbing, baling and transport.

Class	Engine load	Relative frequency	Sample rate error %			
	%	%	5 Hz	1 Hz	0.5 Hz	0.1 Hz
1	0 - 9.99	2.07	0.66	1.80	5.77	42.49
2	10 - 19.99	19.27	0.13	0.37	0.40	4.06
3	20 - 29.99	9.65	0.23	1.62	1.77	5.39
4	30 - 39.99	8.74	0.18	2.18	3.01	7.74
5	40 - 49.99	8.90	0.45	1.90	5.83	18.04
6	50 - 59.99	9.05	0.47	1.55	2.16	6.53
7	60 - 69.99	8.79	0.20	2.93	3.39	9.77
8	70 - 79.99	6.93	0.50	1.73	4.35	13.88
9	80 - 89.99	5.45	0.41	3.03	5.07	7.23
10	90 - 100	21.14	0.10	0.21	0.24	2.49
		100.00	**0.33**	**1.73**	**3.20**	**11.76**

However individual errors per class are much higher than error for total engine load, cf. **Table 9**. While 5 Hz has the lowest average error level of ±0.33 % the other variants have errors of ±1.73, ±3.20 % and ±11.76 %, which is the higest and occures at 0.1 Hz sampling rate. The errors are dependant on relative frequencies in the dataset. The less frequent a class is represented in the original data, the higher the error, especially at low sampling rates. Classes 2 and 10, which have a high representation of 19.27 % and 21.14 % in the data, show low error: ±4.06 % and ±2.49 %. Class 1 represented by 2.07 % in the data has the highest error: ±42.09 %. Although sampling with 1 Hz does not meet the "1 % demand" of Lalanne, errors stay below the reasonable 2 % level.

3.2.4 Description and calculation of attributes

Engine torque is calculated by engine ECU based on actual injection times and engine speed. The information is defined in J1939 and is uploaded via vehicle CAN bus to the data recorder. The resulting so called actual engine percent torque is scaled to the engine nominal torque. Total volumetric fuel consumption was recorded as well.

Overall *gearbox output torque* was directly measured by strain gauges. In addition, the CVT ECU calculates the gearbox output torque based on speed, pump settings and hydraulic pressure. This calculated gearbox torque was also recorded for verification of the strain gauge measured gearbox torque.

The *rear axle torque* is calculated of gearbox output torque and *front axle* drive shaft torque which are both measured by strain gauges. For front and rear axle the further gear ratio to the final drives and the wheel size were taken into account. Also, the efficiencies of the final drives were considered. For the rear axle $\eta_{rear\ axle}$ = 0.95 is assumed which is caused by 5 % losses in the rear axle differential. As for the rear axle, efficiency of the front axle has to be considered which is assumed to be $\eta_{front\ axle}$ = 0.93. The efficiency ends up being 5 % loss for the front axle differential and 2 % for spur gears.

Research from Biller shows less than 45 % of *negative drive wheel torque* level compared to the maximum positive drive wheel torque [24]. Positive torque on the drive

wheel axle is caused by pulling forces during forward operation and push during reverse operation while negative torque is caused by the opposite. As **Figure 32** shows the share of negative drive wheel moments is about 20 %. In this analysis negative torque is not considered. This simplification is possible because both flanks of the gear tooth use the same design, but low loads show significantly lower frequencies [24].

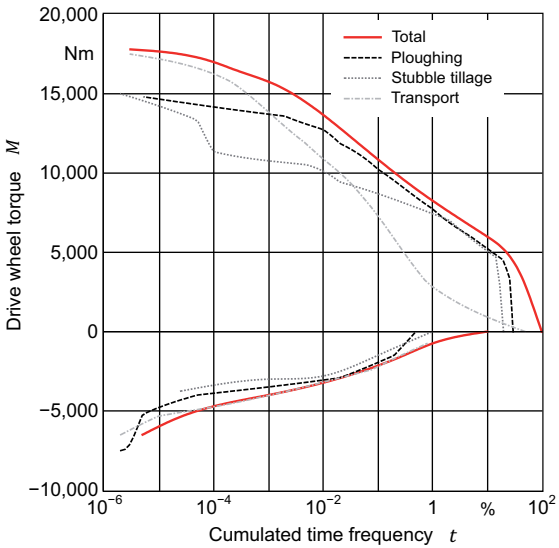

Figure 32: Torque of left drive wheel shaft, loads and low loads for different applications. The Total load spectrum is calculated by weighting of the individual load spectra; from [24].

PTO torque was recorded by external torque measuring hub which used strain gauges as well. Using external measuring devices instead of internal ones reduced the dampening effect of the gearbox and therefore increased accuracy of the measurements.

3.2.5 Classification and interpolation

ISO 6336-6 recommends to calculate service life based on speed synchronous classification [83]. This considers the theory that every load cycle (which means every revolution), damages the gear. Classification based on time has a more general character and can be used for a variety of purposes while speed synchronous classification takes individual machine design into account and reflects real machine stress better than time-based classification.

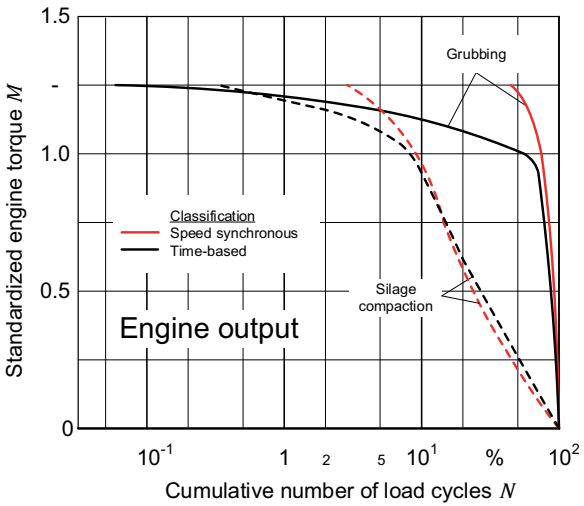

Figure 33: Comparison of time-based and speed synchronous classification of engine torque for different applications.

However, the differences are not that great. In **Figure 33** and **Figure 34** time-based and speed synchronous classification for gearbox input and gearbox output side are compared to each other. On the engine side, it is evident from Figure 33 that for both kinds of applications, heavy pull and silage compaction, speed synchronous classification leads to a heavier load spectrum. This is because high engine torque is mostly achieved at medium to high engine speed and one second at high engine load contributes to more counted revolution in this high torque class than one second at engine

idle speed. The time-based counting method shifts the curve to the right for the lower classes for the same reason. A similar result can be seen on the drive wheel side as well in Figure 34. Speed synchronous classification represents a heavier load spectrum than time-based counting. For low load applications like silage compaction the curves switch but are very similar. A summary of the results in Figure 33 and Figure 34 shows that speed synchronous classification keeps closer to real stress values and also takes drivetrain design into account. That is why it has been chosen

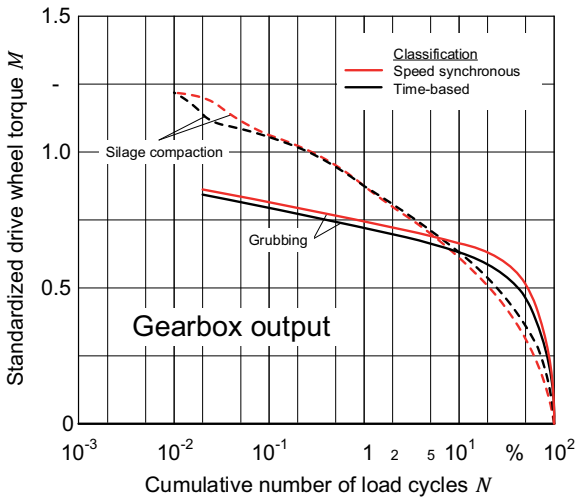

Figure 34: Comparison of time-based and speed synchronous classification of gearbox output torque for different applications.

By means of interpolation, the reference load spectrum which will be described in chapter 3.4.2 is split into equal classes. This procedure fits the reference load spectrum to the classes from the measured load spectrum. The interpolation is done by linear regression to exponential function.

The results of speed-synchronous classification of measurements described in chapter 3.2.1 are shown in **Figure 35**. Engine, gearbox input and PTO are related to engine nominal torque, drive wheel side is related to maximum drivetrain torque.

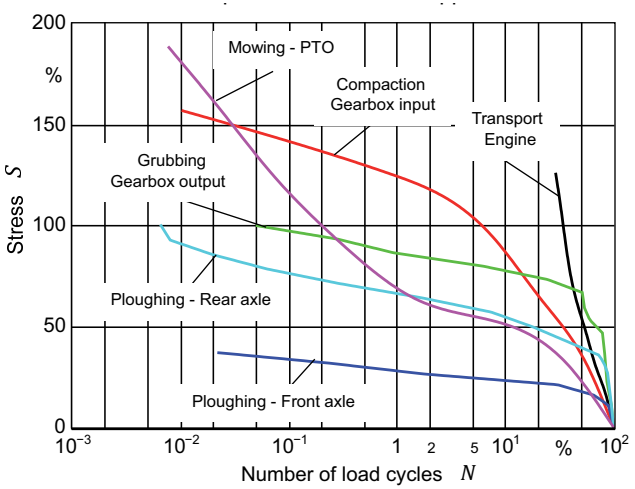

Figure 35: Examples of classified load spectra for different assemblies and applications.

3.2.6 Standardization

The idea of standardization of load spectrum data has been shown in chapter 2.2.5.1 and 2.2.5.2 and enables comparison of data between different tractors and tractor power classes. While the procedure for engine-related load spectra is relatively clear, the subject of how to proceed with drive wheel related load spectra is still being debated.

Engine, *gearbox input* and *PTO* are all related to engine output power and can precisely be described by **Eq.(11)**. The relation to engine nominal torque is generally used as it's a defined point on the engine curve.

$$M = \frac{Torque_{Engine;\ Gearbox\ input;\ PTO}}{Nominal\ torque_{Engine}} \quad \textbf{(11)}$$

Since *gearbox output*, *front* and *rear axle* torque belong mostly to drivetrain design, wheel size and tractor weight, drive wheel force is the value that covers all of these aspects. Renius published an approach which uses these factors to standardize measured torque on the drive wheel side [12]. While the discussion is ongoing whether machine net weight, machine gross weight or a mixture of both is the right means, the author recommends machine net weight. It is a fixed technical value while gross weight or real machine weight is always changing. This fact has to be considered when assembly design is done based on standardized data but is not useful when generating comparable load spectra.

It is assumed that a higher tractor net weight results in higher durability and that tractor net weight increases with tractor size. At the same time larger tractors can produce a higher amount of drive wheel torque due to their weight and wheel size. This means a small tractor producing 10,000 Nm of drive wheel torque and a larger tractor (product of wheel size and net weight two times greater than the smaller one), producing 20,000 Nm of drive wheel force lead to the same standardized drive wheel torque. Taking actual machine weight into calculation would totally influence the standardized torque and underestimate the real situation: A tractor produces 20,000 Nm drive wheel force at a machine net weight of 10 t. By ballasting the tractor with additional 5 t, the resulting standardized torque would decrease by 1/3 without compromising structural integrity (the additional weight coming from front ballast and not from stronger components).

Figure 36 shows quotients from Eq.(9) and Eq.(10) for actual tractor models. A high correlation between tractor class and calculated quotient at low standard deviation is found. The correlation is higher for tractor net weight, $R^2 = 0.91$ than for the average of tractor net and tractor gross weight, $R^2 = 0.89$. For this reason, measured torque on the drive wheel side is related to tractor net weight and tractor standard wheel size. Gearbox output torque was converted to overall drive wheel force (no front wheel assist) by means of **Eq.(12)**. The axles are calculated separately by **Eq.(13)** and **Eq.(14)**.

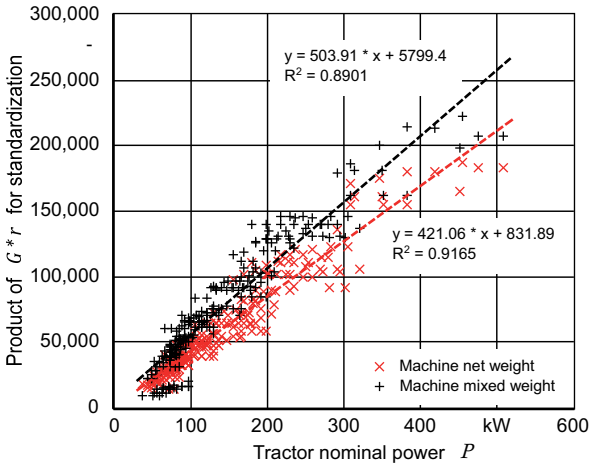

Figure 36: Product of tractor weight (net and mixed weight) for standard and system tractors of the most important manufacturers worldwide, standard wheel sizes, n = 250, 2017.

$$M = \frac{Drive\ wheel\ torque_{overall}}{G_{net} * r_{Drive\ wheel}} \quad \textbf{(12)}$$

$$M = \frac{Drive\ wheel\ torque_{Front\ axle}}{0.4 * G_{net} * r_{Front\ wheel}} \quad \textbf{(13)}$$

$$M = \frac{Drive\ wheel\ torque_{Rear\ axle}}{0.6 * G_{net} * r_{Rear\ wheel}} \quad \textbf{(14)}$$

3.3 Scenario Definition

An overview of the methodic steps to generate a tractor lifetime load spectrum for different assemblies and the definition of different farm types for the scenarios is given in **Figure 37**.

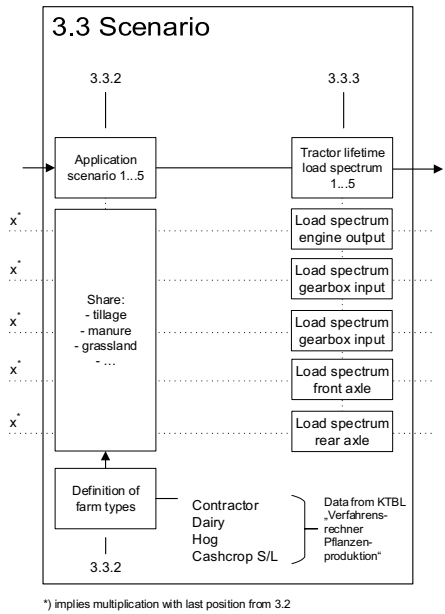

Figure 37: Detailed view of methodic part scenario: from application load spectrum to tractor lifetime load spectrum.

3.3.1 Tractor usage

Tractor utilization varies greatly. An older estimation of tractor usage by tractor power class [11] from 1994 is shown in Figure 4. Since this time, average power per tractor increased which caused a shift in the application spectrum. This increase in tractor power is shown in **Figure 38**. The trend line has an R^2 of 0.95 and shows that an

average tractor in 1994 had 74 kW. 23 years later the average German tractor power in 2017 is 105 kW which equals an increase of almost 45 %.

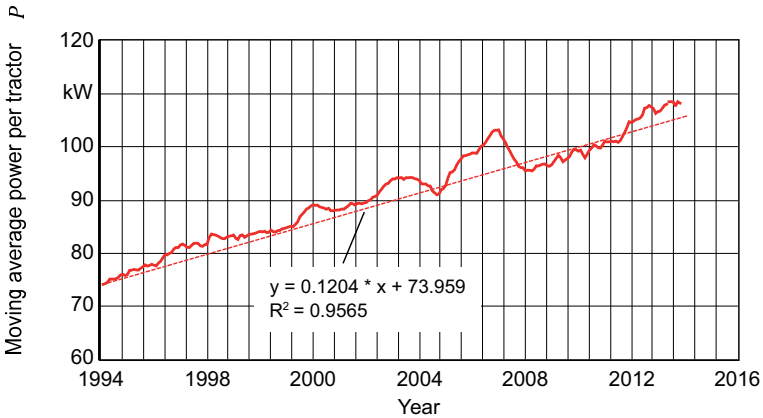

Figure 38: Installed tractor power, 12 month moving average; shipments Germany from VDMA.

Taking this into account, the test tractor positioning is drawn in **Figure 39** with a second axis for tractor power today. The positioning of the test tractor by the adjusted tractor power scale matches the application experiences. This power segment has to fulfill a wide variety of tasks and is still used as front loader tractor. As pointed out by the red marks in Figure 39 the test tractor is at the upper end of a front loader tractor scale but there are still some higher-powered tractors using front loaders. At the same time, it is the tractor segment with the widest variety of applications. Nevertheless Figure 39 shows only annual average tractor application spectrum while different application scenarios for the test tractor are needed.

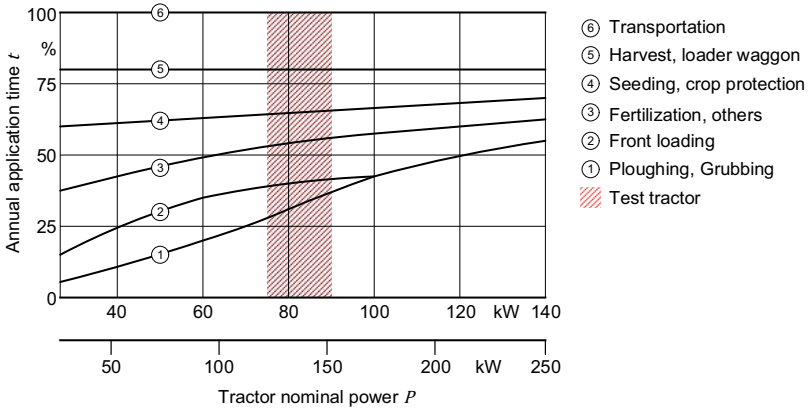

Figure 39: Annual application time for tractors; from [11]. Adjusted power rating based on increasing tractor power from 1994 to 2017 and positioning of test tractor added.

3.3.2 Application scenarios

For validation of the method, different scenarios of tractor lifetime application shall be generated. Based on the previously described average annual applications of tractors within different power classes, **Figure 40** shows the lifetime application spectra of a standard tractor within the 120-140 kW class. The five scenarios use the general farm types which are defined by the BMELV (Federal Ministry of Food and Agriculture) [84] and shall show extremes between the individual tractor usage. The calculation for the usage is based on the farm descriptions from below and planning data from plant production systems from KTBL [85]:

#1 Contractor:

Medium size contractor, > 10 tractors; heavy pull applications are done by larger tractors; silage compaction is done by larger tractors. Typical applications: crop care, grassland incl. baling, seeding and transport. No ploughing or grubbing.

#2 Dairy:

80 ha; tractor is the largest tractor and does most of the work; 120 cows, self-

mechanized: grassland applications, slurry, silage compaction, no arable farming which means no ploughing or grubbing.

#3 Hog:

80 ha, 1,500 hogs; tractor is the largest tractor and does most of the work; self-mechanized: slurry, crop care, ploughing, grubbing and seeding.

#4 Cashcrop small:

150 ha, crop rotation: WW-WR-SG; no organic fertilization, 3x tillage, 3x crop protection on average; tractor is the largest tractor and does most of the work, including ploughing and grubbing.

#5 Cashcrop large:

1,500 ha, crop rotation: WW-WR-SG; tractor is the smallest tractor and does only crop care and fertilization, transport and seeding; no ploughing or grubbing.

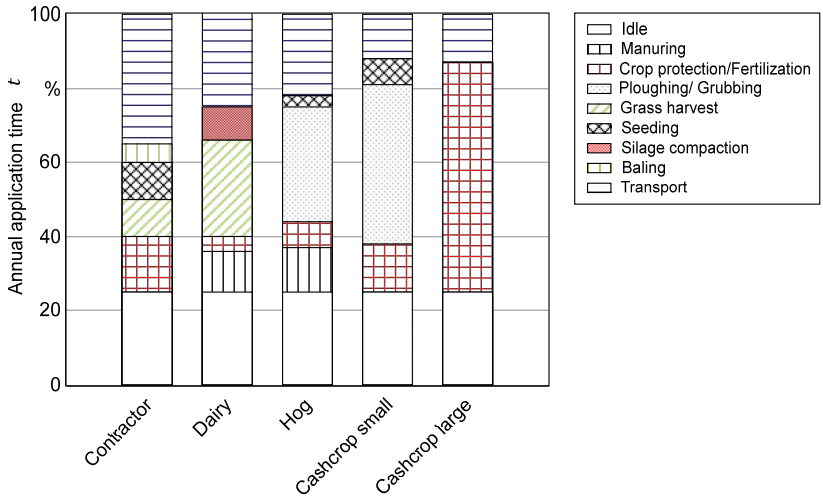

Figure 40: Stacked annual application times of standard tractors for five different scenarios as defined as typical farms, tractor power range 120-140 kW.

While Figure 40 shows the applications based on the scenarios **Table 10** lists the resulting application spectrum based on the measurements. Because there is no load spectrum data for all applications available, the data which comes as close as possible was chosen. Although Table 10 only shows the share of different applications, it seems to be relatively clear that scenarios with a high share of tillage will lead to high load on the tractor while lighter applications such as greenline or transportation puts lower loads on the machine.

Table 10: Application spectrum for different scenarios, #1 contractor, #2 dairy, #3 hog, #4 cashcrop small, #5 cashcrop large.

	Scenario				
%	**1**	**2**	**3**	**4**	**5**
Tillage	-	-	35	50*	25*
Slurry	-	10	10	-	-
Manure	10	5	-	5**	10**
Greenline	15	30	-	-	-
Baling	5	5	-	-	10
Transport	35	25	25	20	30
PTO others	10	-	5	-	-
Idle	25	25	25	25	25

* includes seeding

** instead of lime spreading

3.3.3 Tractor lifetime load spectra

The tractor lifetime load spectra which are shown in **Figure 41** and **Figure 42** have been calculated on the basis of Table 10. The left side shows engine side related load spectra as *engine output* and *gearbox input* in standardized engine torque. The right side shows drive wheel related load spectra as *gearbox output*, *front* and *rear axle* in standardized drive wheel torque.

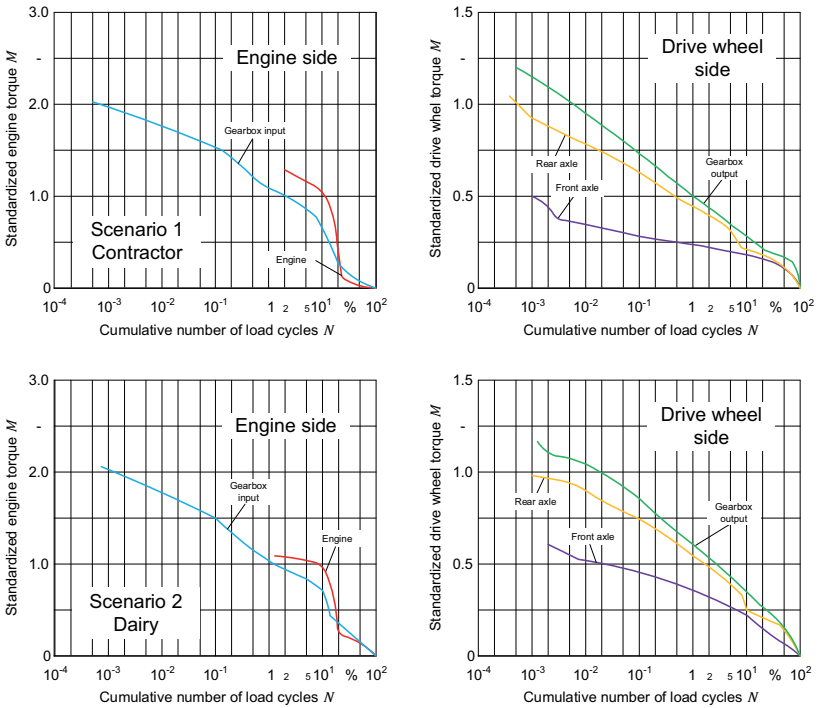

Figure 41: Tractor lifetime load spectrum for scenarios #1 contractor and #2 dairy, engine and drive wheel side.

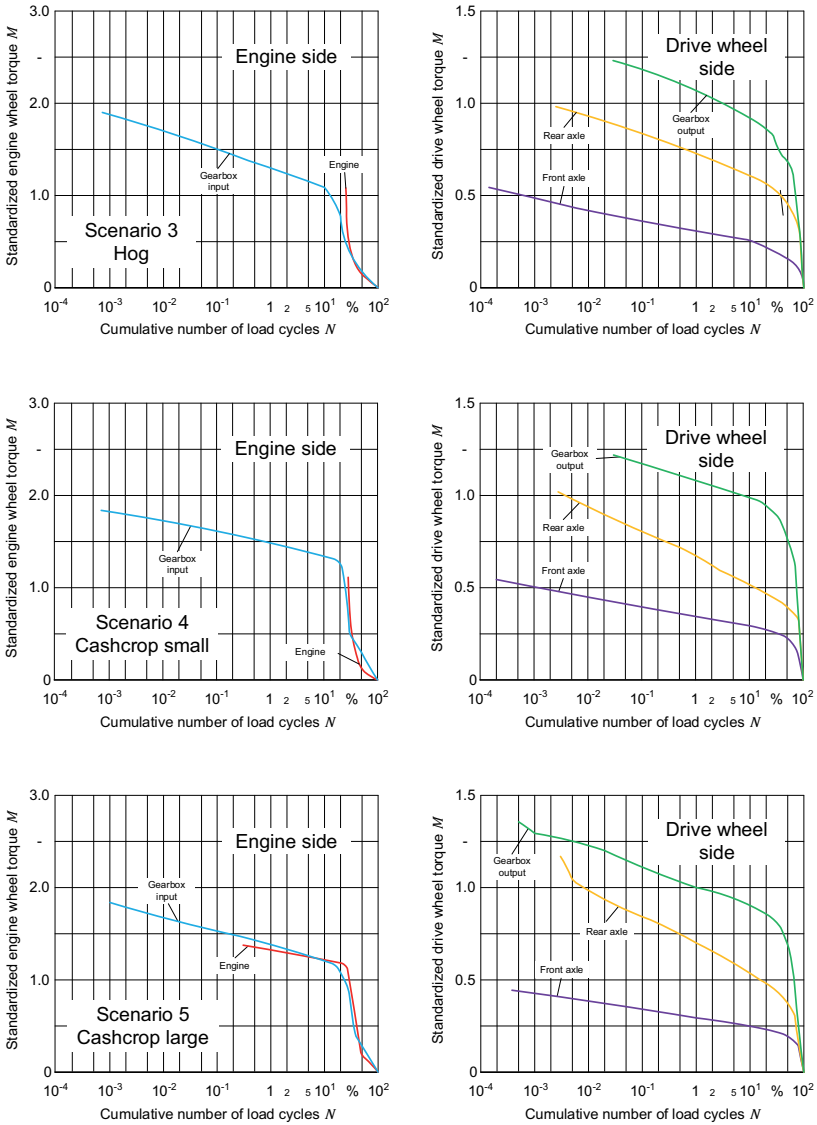

Figure 42: Tractor lifetime load spectrum for scenarios #3 hog, #4 cashcrop small and #5 cashcrop large, engine and drive wheel side.

3.4 Load calculation

The necessary steps for calculating assembly-specific load sums for tractor lifetime load spectrum and reference load spectrum are shown in **Figure 43** as well as the deduction of the reference load spectra.

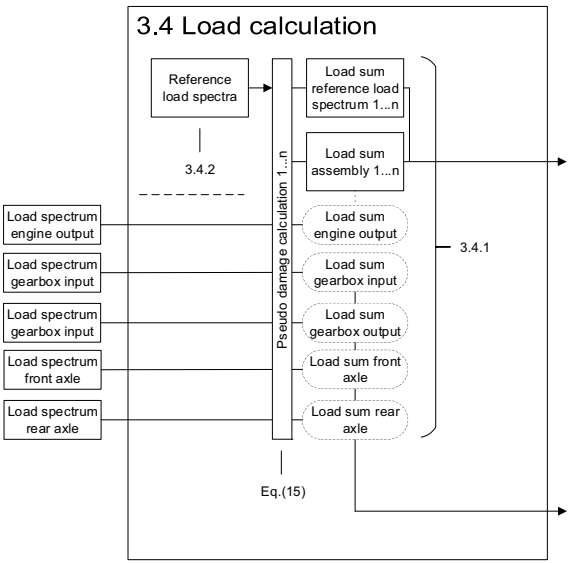

Figure 43: Detailed view of methodic part load calculation: from tractor lifetime load spectrum to load sums, deduction of reference load spectra.

3.4.1 Pseudo damage calculation and load sum

While single stage tests can easily be compared to each other, load spectra cannot be compared directly because they are not a single stage test. For comparison damage accumulation hypothesis is required as mentioned in 2.2.1. But Wöhler curves depend on a lot of different factors and are almost unique and very hard to achieve the more complex the assemblies' design gets. **Figure 44** shows different exemplary Wöhler curves for an assembly for tooth root, tooth flank, bearing and shaft. It points out the complexity of precise damage calculation. As gearboxes do not consist of one shaft

and one bearing and also not every gear, shaft or bearing is engaged and loaded with stress all the time it would be an enormous effort to calculate single component and subcomponent damage separately. There are different possibilities to take all the different curves into consideration. For example the minimum of all or an average of the curves. But this would make the approach more precise as possible only for a single machine. Nevertheless by using a hypothetical Wöhler curve (h) with overall slope exponent k = 5 from “FKM-Guidline” (Research Curatorship for Mechanical Engineering) [86] a good indication of past stress can be calculated for the overall assembly.

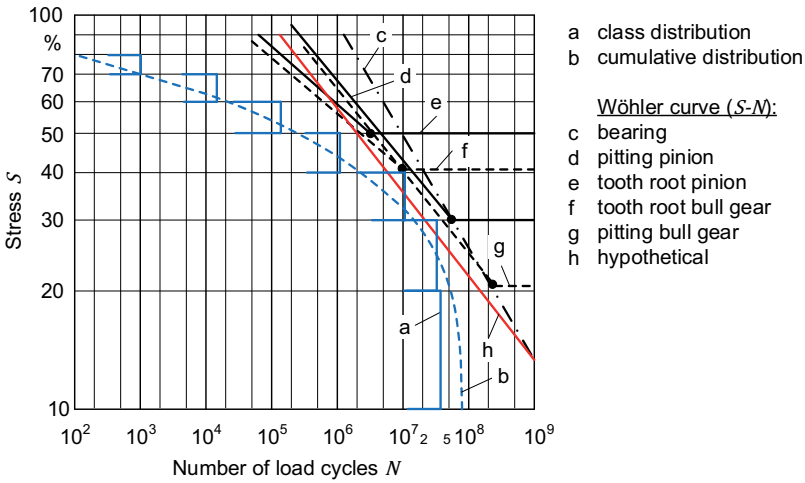

Figure 44: Class distribution of loads and Wöhler curves for different components within the drivetrain with hypothetical Wöhler curve; edited from [23].

The pseudo damage calculation works similar to the Miner’s rule which has been described in chapter 2.2.1. The number of load cycles n of the measured load spectrum is compared at class mean to the hypothetical Wöhler curve (h) which gives the potentially possible number of load cycles N by means of Eq. (1). Summing up the class individual loads by **Eq.(15)** the load sum L is calculated. L is generated separately for every assembly.

$$L = \sum_{i=1}^{k} \frac{n_i}{N_i} \quad \textbf{(15)}$$

Load sums are calculated for the reference load spectra as well as for the measured tractor lifetime load spectra.

3.4.2 Reference load spectra

A standardized load spectra for a standard tractor is described in chapter 2.2.4. This is used as a basis for derivation of assembly specific reference load spectra. The original curve is interpolated according to the descriptions in chapter 3.2.5 to fit individual class mean from measured load spectra.

3.4.2.1 Engine

Existing engine load spectra are described in chapter 2.2.5.1. These were measured and developed for standard tractors without front wheel assist and manual shift transmission. As shown in Figure 14 peak loads are mainly caused by clutch operation and gear shifts. The suggested load spectrum is listed and compared to the published load spectrum in **Table 11**.

Table 11: Engine reference load spectrum, original and adapted, listing by Renius definition from [12], maximum torque adapted.

		Distribution	Renius 1976	Suggestion
		% n	Standardized torque*	
Lower end	**I**	100	0	0
Central point	**II**	50	0.76	1.16
Maximum torque	**III**	4.5 | 3.0	1.08 - 1.15	1.4
Peak load	**IV**	0.0033	2.5	-

* Eq.(11)

The suggested engine reference load spectrum is presented in **Figure 45**. Both curves start at 100 % and 0 torque. CVT is integrated more deeply into tractor drivetrain management than the manual shift gearbox in 1976. Drive controller adjust the transmission ratio in a way to droop the engine to its most efficient point. For this reason the distribution of the engine load spectrum changed to nearly 50 % higher torque levels at the central point of the load spectrum. Modern engines have other torque behavior which leverages the point of maximum torque to 140 % of standardized engine torque at 3.0 % frequency. Because the test tractor uses a CVT, which runs much smoother, because clutching and speed adaption between engine and gearbox input side is done by hydraulic swash plate pumps, the suggested engine load spectrum is cut at 140 % of standardized engine torque.

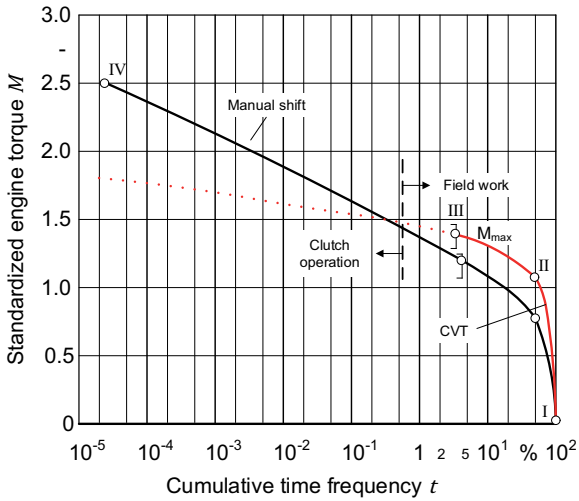

Figure 45: Reference engine load spectrum of manual shift tractors; from [12]. Additional red curve indicates engine reference load spectrum for CVT tractors. The dotted line is a projection similar to the black curve. The roman numbers indicate important positions for load spectrum calculation.

3.4.2.2 Gearbox input

Load spectrum for engine output and gearbox input are very similar as long as the whole engine power output is transferred to the drivetrain. Rear-PTO can consume a high portion of engine power output, but time of engagement during tractor lifetime is on average below 10 %. Tractors are rarely equipped with front-PTO and the activation time is even lower than for the rear-PTO. For these reasons PTO is not considered for gearbox input load spectrum. Additional losses from engine to gearbox are caused by auxiliaries:

- Cooling fan
- Alternator
- Air conditioner
- Air compressor
- Hydraulic pump for break.

Pichelmaier published losses for a special 3-axle tractor design under heavy pull conditions [30]. These have to be adjusted to a standard MFWD tractor. The assumed losses are displayed in **Figure 46**. In total auxiliaries end up with 26 % peak losses. During tractor lifetime the amount of power consumption varies greatly.

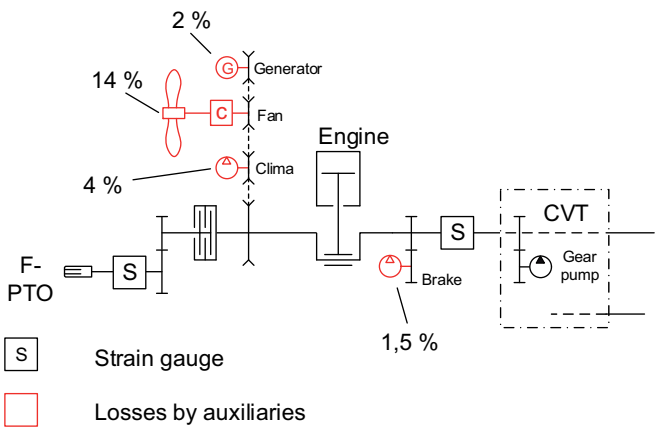

Figure 46: Power losses for a 3-axle tractor (387 kW nominal power) with double engine concept from engine to CVT gearbox during grubbing, working speed 9 km/h, working depth 20 cm; losses edited from [30; 79].

Analysis of the measurements in **Figure 47** shows 10 - 12 % losses between engine output and gearbox input on average. For this reason, a general loss of 10 % between engine output and gearbox input is assumed. This means that generally, tractor engine power measured at rear PTO should not result in more than 10 % losses in comparison to rated tractor nominal engine power.

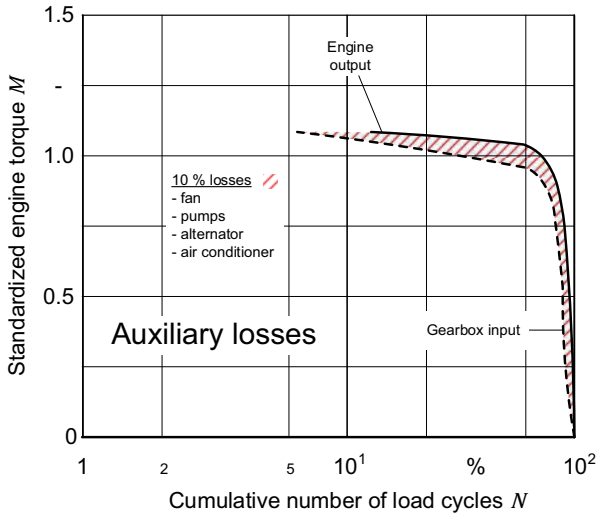

Figure 47: Average power losses during heavy pull applications between engine output and gearbox input due to auxiliaries, indicated by the hatched area.

3.4.2.3 Gearbox output

Load spectrum for drive wheel side has been published by Renius [12]. The original load spectrum, the black curve in **Figure 48**, fits well to heavy pull applications but is too hard for tractor lifetime reference. The suggested red curve for gearbox output of CVT tractors equals 80 % of the original load spectrum. This means that the load distribution stays the same but stress level is reduced to 80 %.

The measured gearbox output torque is virtually transformed in standardized rear drive wheel torque. Because the measured torque at gearbox output is in focus, losses further down the drivetrain are not considered. This allows the comparison to the black curve which was measured directly at the drive wheel of a tractor without front wheel assist.

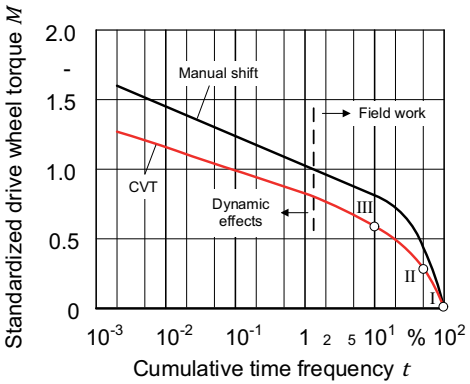

Figure 48: Reference gearbox output load spectrum for manual shift tractors; from [12], additional red curve adapted for gearbox output load spectrum of CVT tractors.

In Figure 48 the original gearbox output load spectrum and the adapted one for CVT tractors is shown. Numbers I to III are defined in chapter 2.2.5.2. The dashed line indicates the split point between “static” and “dynamic” loads. While “static” loads are mainly generated by field operation and can hardly exceed 1.0, the points above are caused by load peaks due to manual shift or environmental effects such as soil compaction. 1.0 marks the point of maximum driving force of front wheel assist tractors on an underground with driving force coefficient κ = 1.0. Higher drive wheel torque can only be generated due to dynamic effects or transfer of down force from implement to tractor. For the CVT curve this point is shifted to the left side of the diagram. According to Renius the 10 % point of a drive wheel side load spectrum marks the static point of heavy pull operations like ploughing. For the suggested load spectrum this point equals κ = 0.5 which is a realistic value on average for most of the soils [87; 88]. Under heavy pull conditions, CVT tractors show a load spectrum which is shifted more to the right.

Up to the 1 % point the curves stay above the suggested reference. Due to an engine transmission control, CVT tractors reach higher torque for a higher portion of time. The front wheel assist also increases driving force because the whole traction potential is used instead of using just the rear drive axle as is the case for tractors without front wheel assist. However, the original load spectrum is too heavy in comparison to the measurements done with the test tractor and is reduced for this reason.

3.4.2.4 Axles

The original load spectrum was published for a standard tractor without front wheel assist. Modern standard tractors in Europe are mostly equipped with front wheel assist. Depending on the application, soil condition and driving speed the front axle drive can be engaged or disengaged. When the front axle drive is disengaged, power split in drivetrain behaves as has been measured by Renius. In these cases, the load spectra are comparable. When the front axle drive is engaged, power is split between rear and front axle analog to weight distribution. Because this is statically influenced by counterweight and mounted implement, and dynamically influenced by soil and operating speed an overall weight distribution of 40 % front axle and 60 % rear axle is assumed which equals static axle weight distribution during most of the field operations of the test tractor.

For the *rear axle* the reference load spectrum for gearbox output from chapter 3.4.2.3 is used and multiplied by static axle load distribution. For a comparison of the measured rear axle load spectrum with the reference load spectrum, the axle efficiency has to be taken into account. Drive wheel torque is standardized by Eq.(13).

Front axle load spectrum refers to Meiners [36], who published front axle load spectrum for field and front loading operation. This given load spectrum is also reduced by a factor of 0.8 so that overall load distribution is the same, but stress levels are reduced. The front axle torque is standardized by Eq.(12) and the assumed front axle weight distribution of 40 %. Furthermore, none of the test results showed the same rare load peaks - loads left of 10^{-3} % frequency. The assumed front axle reference load spectrum is cut for this reason at this point. Both reference load spectra are displayed in **Figure 49**.

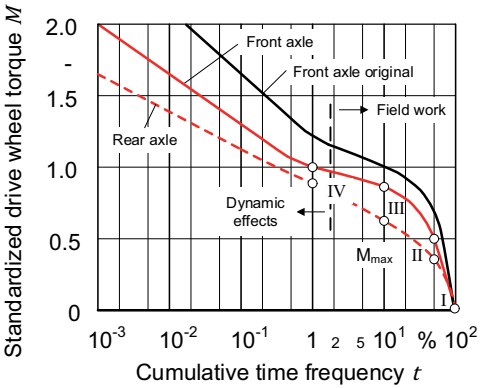

Figure 49: Reference front axle load spectrum for manual shift tractors, from [36], the additional red curve is adapted to CVT tractors. The dotted red curve shows rear axle reference load spectrum for CVT tractors; adapted from red curves from [12].

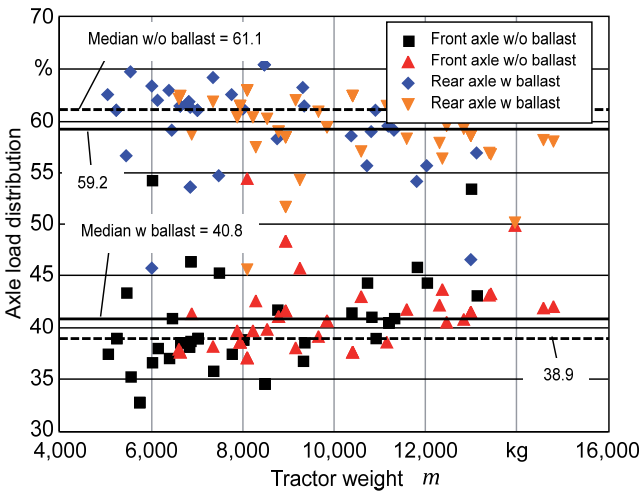

Figure 50: Axle load distribution for unballasted and ballasted standard tractors, straight line indicates median of ballasted tractors and dotted line for unballasted tractors (upper lines for rear axle, lower lines for front axle), technical data from western tractor OEMs, n = 47.

This axle weight distribution is confirmed by **Figure 50** which shows a ratio of un-ballasted rear axle weight of 61.1 % and ballasted tractor weight ratio of 59.2 %. The data is based on 47 tractors which were measured by the DLG for the powermix test [89].

3.5 Evaluation

The final evaluation of the damage sums can be made using the relation to standard operation hours or direct comparison to other tractors, which is described in **Figure 51** in detail.

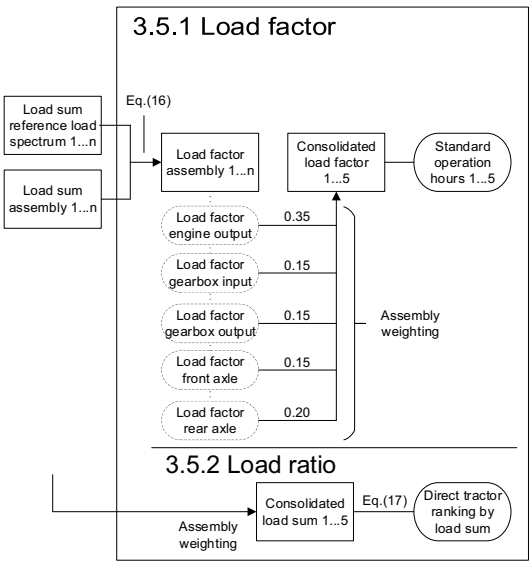

Figure 51: Detailed view of methodic part load factor: from load sums to standard operation hours or alternatively direct tractor ranking.

3.5.1 Load factor

For the calculation of the load factor (LF) of an operation hour the ratio of tested load sum L_{Test} and the reference load sum $L_{Reference}$ has to be calculated by means of **Eq.(16)**. This is done for each assembly. At this point detailed tractor evaluation is possible for each assembly.

$$LF = \frac{L_{Test}}{L_{Reference}} \quad \textbf{(16)}$$

For consolidation of the individual load factors to one overall tractor load factor, assemblies are weighted by their individual retail price ratio. All load factors are multiplied by the weight factors, which are shown in Figure 51, and are summed up. This overall load factor can be used to evaluate the tractor operation hours. Therefore, the operation hours from the hour meter are corrected by the load factor. The resulting hours equal standard operation hours, which in this case, are related to the reference load spectra suggested in chapter **3.4.2**. In addition, tractors can be directly compared at different points in their 10,000 h. This method provides an “absolute” indication of tractor stress and allows an evaluation of the economy of specific machine.

3.5.2 Load ratio

To make a comparison of different tractors within a certain power range, another calculation has to be done. First the assembly-specific load sums have to be consolidated. This is described in **3.5.1**. The resulting overall tractor load sum $L_{Tractor\,A}$ can be directly compared to another tractor $L_{Tractor\,B}$ by means of **Eq.(17)** and is called load ratio (LR). Because the real past loads are relevant for tractor evaluation, it is not necessary to reference the LR to operation hours. A tractor with low operation hours will generally have a lower load sum than tractors with higher operation hours on their meter. This results in a lower LR. This method shows the relative advantage or disadvantage in comparison to at least one other tractor and can never be considered on its own.

$$LR = \frac{L_{Tractor\,A}}{L_{Tractor\,B}} \quad \textbf{(17)}$$

3.6 Simplification of measurement

The test tractor was equipped with a variety of additional sensors which are not state-of-the-art in tractor series production and which increase the cost of the machine. The types of sensors and measuring set-up is described in chapter 3.2.2. This extra information allows an analysis of whether the same information can be gathered by using more global vehicle controller area network (CAN)-Bus data.

To do this, calculated load factors are compared with:

- Engine fuel consumption
- Engine torque load by engine electronic control unit (ECU)
- Engine fuel consumption corrected for average engine speed
- Gearbox input torque for pull only applications.

By comparing fuel related parameters, the question of whether or not strain gauges are redundant and can be replaced by data gathered from engine ECU, can be answered. By comparison of ECU engine output torque and strain gauge measured gearbox input torque and gearbox ECU torque the signals are analyzed for their accuracy in belongings of torque peaks.

4 RESULTS AND DISCUSSION

4.1 Tractor lifetime load spectrum

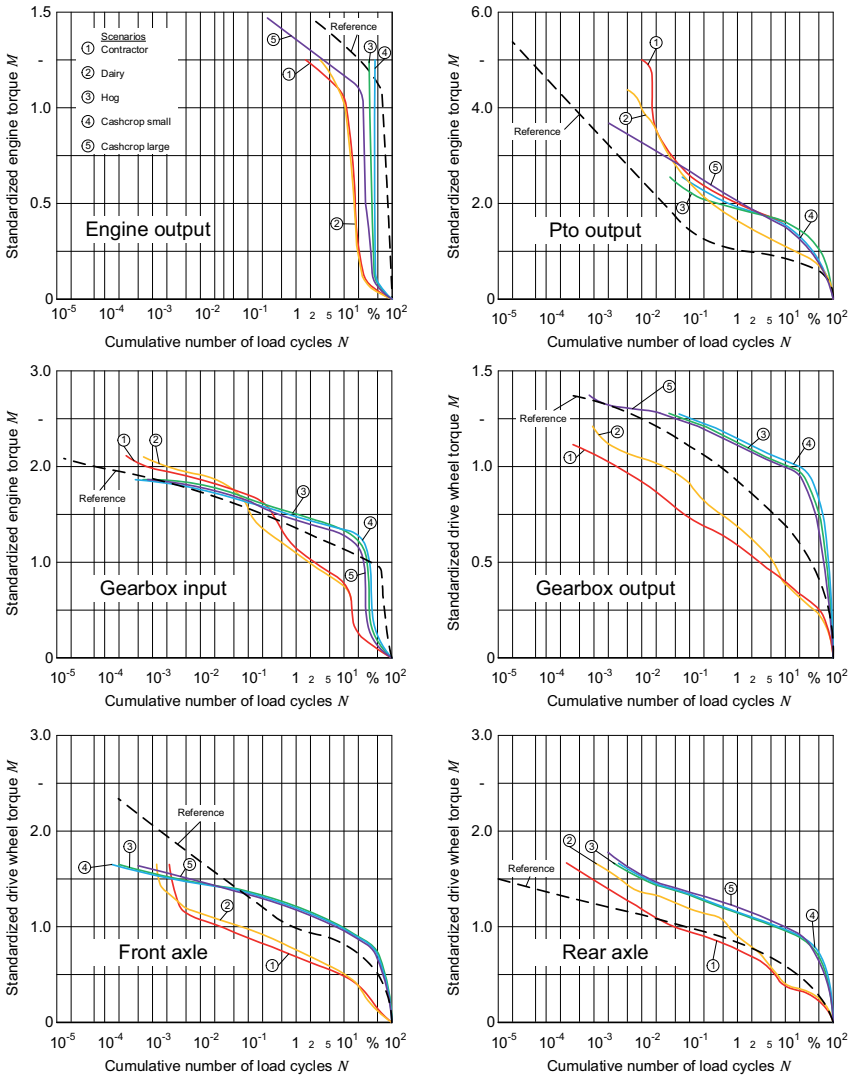

Figure 52: Assembly specific load spectra for different tractor lifetime application scenarios #1 contractor, #2 dairy, #3 hog, #4 cashcrop small, #5 cashcrop large. The black dotted line indicates the reference load spectra from 3.4.2.

After applying the described method, the lifetime load spectra shown in **Figure 52** are the basis for the further discussion. The references from chapter 3.4.2 are added to the load spectra for a better overview. Data in the plot is standardized by means of Eq.11 - Eq.14. The number of the curves corresponds to the number of the scenarios from 3.3.2:

#1 Contractor
#2 Dairy
#3 Hog
#4 Cashcrop small
#5 Cashcrop large.

4.1.1 Engine

Figure 53 presents the engine lifetime load spectrum in detail. It shows engine ECU calculated output torque in relation to engine nominal torque. The engine ECU estimates output torque by injection time, actual engine speed and internal friction, which is stored as a correction function on the engine ECU. In contrast to all other plots, the engine output load spectra does not vary greatly. Frequencies below 1 % can only be observed for curve #5 which ends close to 150 % of engine nominal torque at 0.30 % frequency. Curves #1 and #2 show almost the same characteristics, with curve #2 showing slightly higher frequencies at the upper end. The general distribution of curves #1, #2 and #5 is very similar and shows a characteristic knee point slightly above 100 % engine torque. This knee point comes from the engine transmission management which adjusts the transmission ratio to drop the engine to a fuel-efficient operation point at high torque.

In comparison, the curves #3 and #4 keep above the curves #1, #2 and #5 and turn vertical below the 50 % frequency. Both curves end at the same level of #1 and #2 at engine maximum torque. According to Table 10 the scenarios behind #3 and #4 are characterized by the high amount of tillage. For these applications the complete engine torque is required constantly. This explains the missing knee point to load peaks at 10 - 20 % as curves #1, #2 and #5 show. The main reason for the missing knee point

is the lack of sensor data for engine output torque. Engine ECU only calculates torque up to engine maximum torque and cuts off torque peaks above.

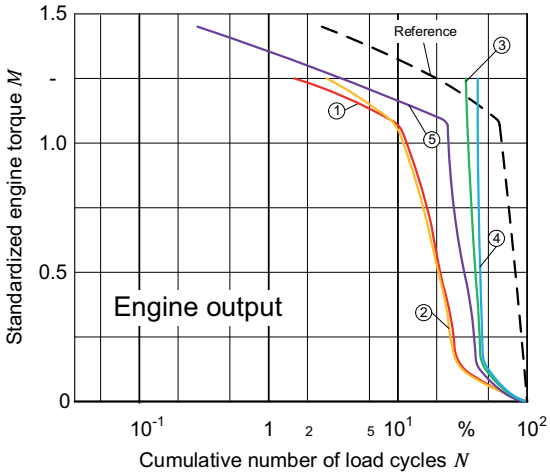

Figure 53: Engine load spectra for different tractor lifetime application scenarios, #1 contractor, #2 dairy, #3 hog, #4 cashcrop small, #5 cashcrop large. The black dotted line indicates the reference load spectra from 3.4.2.

The curves #3 and #4 are the only curves that cross the engine reference while all others stay below the reference. Taking the basics of fatigue and pseudo damage calculation into account the scenarios should cause low load factors for curves #1 and #2, a medium load factor for curve #5 and the highest load factors for curves #3 and #4.

The method of pseudo damage calculation is used to evaluate the engine as well although damage mechanisms vary for engines in comparison to pure mechanical assemblies such as gearboxes or axles. Based on the MAN patent [66], weighting factors for the specific operation points would be sufficient but nowadays none of the engine manufacturers published the necessary information.

4.1.2 Gearbox input

The middle left plot in Figure 52 shows results for the gearbox input side. Because of the lack of gear shifts or clutch operation in CVT tractors the general distribution is relatively smooth and close to engine output curves. Curves #1 and #2 reach about 200 % engine nominal torque at 10^{-3} % frequency, curves #3 - #5 stay at lower torque levels. Nevertheless, this diagram shows the previously described problematic of using calculated ECU values instead of strain gauge measured ones. While curves #3 and #4 do not show a knee point on the engine output side they do have a knee point on the gearbox input side because of the different measuring principle.

Two general distributions can be characterized in the plot. While curves #3 - #5 follow the engine output, curves #1 and #2 have another distribution. They stay above large sections of the load spectrum below curves #3 - #5 but cross them at the end. The gap between the curves between 50 % frequency and 0.5 % frequency is caused by power consumption for other components within the tractor. Because auxiliary losses do not vary greatly over a tractor lifetime load spectrum, the difference is caused by PTO operation. Table 10 shows 40 % PTO applications for curve #1 and 50 % for curve #2. While curves #3 - #5 use the biggest portion of engine output torque for driving #1 and #2 do also use some amount for PTO. The lower amount of PTO work or PTO power consumption for curves #3 - #5 is expressed by the slightly bigger gap between the curves and the reference right from the start.

None of the curves reaches loads above 200 % engine nominal torque although the older sources show such high peak loads. The original source from Renius [12] used a manual shift, clutch operated, rear wheel driven tractor for measurements. The upper part of the load spectrum was calculated based on the idea of single hard clutching events and the clutch maximum friction torque of 250 %. A CVT tractor is not equipped with such a clutch and is operated in another way. Gears are shifted automatically and much smoother, there are hardly any high torque peaks on the gearbox input side, caused by gear shifts.

All curves cross the gearbox input reference curve. By means of pseudo damage calculation the resulting load factors should build two groups. Curves #1 and #2 have lower load factors than curves #3 - #5.

4.1.3 Gearbox output

The gearbox output load spectra are shown on the middle right plot in Figure 52. Standardization is done by means of Eq.(12). Although the chosen reference is from 1976 [12], general distribution is still valid. While curves #3 - #5 are more bulbous than the reference, curves #1 and #2 are straighter. This is caused by the engine transmission management system which sets transmission ratio in a way that engine speed is drooped to a point of high efficiency and high output torque. In contrast to the original load spectrum for the rear axle which had a more equal distribution, the curves #3 - #5 have a higher amount of time at high load levels. This is expressed by the steep start from 100 % to 20 % where the knee point of the curves is located. Below 20 %the curves show less incline. The heavy load scenarios #3 and #4 show the highest torque level except of the load peaks from curve #5. Relative frequencies stay below 125 % standardized drive wheel torque at 0.05 % relative frequency for #3 and #4. The other curves show load peaks up to 10^{-3} % between 110 % and 130 % of standardized drive wheel torque.

The reference equals 80 % of the original load spectrum. The reduction was done because only heavy pull applications such as tillage came close to the original load spectrum for the drive wheel. This is due to three factors:

1. The standardization method which takes machine net weight into consideration: Because the test tractor has a relatively high net weight in comparison to the engine power, all measured torque peaks were divided by the high net weight and resulted in a lower standardized drive wheel torque.
2. For the original drive wheel reference load spectrum, the measurement was done closer to the tire-soil contact than in the test tractor. The strain gauges were positioned directly behind the gearbox output and on the drive shaft to the front axle. In the current measurements wheel forces of the test tractor were calculated and not measured directly in the drive wheel.
3. Original measurement was done on a standard tractor without front wheel assist. This kind of tractor do not use the full tractor pulling-force potential because the remaining driving potential of the front axle is not used to generate traction. The overall generated torque within the drivetrain of these tractors is lower than for the tested tractor which used front wheel assist most of the time.

Two curves, #1 and #2, stay below the reference. Both have more non-driving force related applications in their load spectrum, for example transportation, greenline or stationary PTO operation. Thus, both show less load cycles at high drive wheel torque levels.

All curves do not angle directly to the left from the 100 % point on the right bottom of the plot. This is because both engine side plots, engine output and gearbox input load spectra, are fully affected by the amount of idle time while the drive wheel side usually stands still during idling. Idling makes up to 25 % of tractor operation time [1]. During this time the tractor engine runs at 900 min^{-1} at very low loads and tilts the load spectrum to the left side. Because the drive wheel side usually stands still during idle, the gearbox output load spectrum does not change as classification is done speed-synchronous. Figure 52 shows relative number of load cycles. In an absolute plot gearbox output distribution would be the same but completely shifted to the relating 75 % point in terms of number of load cycles.

4.1.4 Axles

The lower left of Figure 52 shows the front axle load spectrum which is standardized by means of Eq.(13), the lower right shows the rear axle load spectrum which is standardized by means of Eq.(14). Because of this individual standardization, the load spectra of rear axle and front axle cannot be summed up to a 100 % cumulative frequency load spectrum for gearbox output. Further effects such as recirculating torque during reverse push operation (e.g. pushing silage on the silage bin) can exceed the weighted gearbox output torque. Similar effects come from tension due to forerun of the front axle on surfaces with high μ.

The *front axle* load spectrum behave relatively smoothly and keep to the original drive wheel curve distribution for rear axles from Renius [12]. Nevertheless the front axle field load spectrum from Meiners, published in 1984 [36], is used as front axle reference. Because the original curve showed higher loads than those achieved during any measurement, the curve was reduced to 80 % of the original curve, analog to the gearbox output load spectrum reference from Renius. Measured loads are calculated based on front axle net weight distribution and front wheel size. Because both are

smaller than the numbers for gearbox output or rear axle the quotient for standardization decreases and calculated standardized drive wheel torque reaches equal loads than rear axle.

The load spectra show peaks up to 160 % standardized drive wheel torque at 10^{-3} % for the curves #1 and #2 and slightly less common peaks at the same load level at frequencies of $5*10^{-4}$ to $1.5*10^{-4}$ for curves #3 and #4. Two types of load spectra can be characterized. The higher loads are shown by curves #3 - #5. Up to the 1 % point their frequency distribution is close to the reference. Below the 1 % point #3 - #5 show decreasing incline. The curves #1 and #2 keep below the reference which is the result of applications with low demand for front-wheel assist driving power. Transportation is one example for applications, where front-wheel assist is only partly engaged during breaking. Over the range of 10 % to 10^{-2} % all curves have almost the same slope but #1 and #2 show steep ends. These are caused by peak loads which are generated by applications such as silage compaction. During silage pushing and compaction the front axle drive wheel load is low most of the time, but it increases dramatically when pushing the silage up to a silage bin.

While the scenarios #1 and #2 stay below the reference, curves #3 - #5 cross the reference at 0.1 % and 120 % standardized drive wheel torque. The resulting load factors should behave in the same manner. Meiners' reference for front axle during field operation still exceeds the heaviest measurement on the test tractor. This reached 160 % standardized drive wheel torque in comparison to 240 % according to Meiners. Again, measurements were done with a manual shift clutch-operated tractor which explains the steeper curve from the 1 % point. At this point field operation influence ends and dynamic and shift effects begin.

The *rear axle* load spectrum shows similar characteristics for the curves #3 - #5 like the Renius drive wheel load spectrum from 1976 [12]. The curves #1 - #4 reach loads up to 160 % standardized drive wheel torque at $3*10^{-3}$ to $3*10^{-4}$ % cumulative frequency while #5 exceeds it slightly with 175 % at $2*10^{-3}$ % frequency.

The reference curve is based on the reduced drive wheel load spectrum (which is explained in chapter 3.4.2.3) and rear axle net weight distribution and wheel size (see chapter 3.4.2.4). This causes a higher standardization quotient than for the front axle so that standardized loads show almost the same load levels as front axle, e.g. #3 - #5

front axle in Figure 52 bottom left. The PTO- and transportation-influenced scenarios #1 and #2 show a bulbous line to the left side around the 10 % point, which comes from low load applications such as transportation, mowing or silage compaction.

While #1 and #2 start below the reference load spectrum and cross the reference at 2 % frequency and 75 % load, #1 or #2 cross at $3*10^{-3}$ and 100 % standardized drive wheel load. The other curves stay above the reference right from the start. This indicates high load factors on the rear axle for all scenarios, especially for #3 - 5.

4.1.5 PTO

In addition, Figure 52 shows the results from rear PTO measurement. PTO was not taken into account for the calculation of the following encompassing load factor in chapter 4.2, but it was considered for load ratio comparison in chapter 4.3. Standardization has been done based on engine nominal torque by means of Eq.(11). PTO reference load spectrum is taken from Meiners (Meiners hard) [36].

Up to the 0.1 % point, curves show almost equal distribution characteristics, but peak loads depend a lot on the chosen scenario. While #3 and #4 show loads of 250 % of engine nominal torque at 0.1 to 0.05 %, curve #5 ends at 360 % load at $2*10^{-3}$ %. Scenario #1 and #2 show peaks around 10^{-2} %, at #2 420 % and #1 500 % engine nominal torque. The scenario is mainly influenced by heavy PTO operation such as square baling and corn milling. The interaction with extremely heavy centrifugal forces on implements, especially during their engagement causes high load peaks. Also, the oscillating piston for compression of the straw or grass material causes highly dynamic loads. Scenario #2 is more influenced by mowing and baling. Because mowing has a high-power consumption on the PTO but runs with less load peaks the curve is smoother.

All curves stay above the reference load spectrum. #2 keeps closer to the reference, #3 - #5 end closer to the PTO reference curve. The PTO load spectra vary greatly for different application scenarios which makes comparison to Meiners difficult.

Tests showed load factors up to 25 due to the big gap to the reference load spectrum. A simple lift of the curve was not possible because general frequency distribution did not match the curves at all. For this reason, PTO was not considered for load factor calculation. Nevertheless, the gap between all curves and the reference curve indicates generally higher loads on the PTO drivetrain in comparison to the measurements published by Meiners. An increase of the reference curve by 200 % from 100 % engine nominal torque at 1 % frequency to 200 % is suggested but not tested so far.

4.2 Load factor

The following load factors compare the lifetime load spectrum of the individual assemblies to a reference load spectrum for the specific assembly. The reference load spectra are described in chapter 3.4.2 and are equivalent to a standard operation hour. **Table 12** shows the resulting load factors for the different scenarios #1 - #5. Assuming 10,000 h of tractor lifetime, the LF have to be interpreted as follows: #1 engine LF is 0.21 which means the engine's operation hours equal 2,100 standard operation hours. Gearbox input scenario #4, LF 1.65 equals 16,500 standard gearbox input hours. While the resulting standard engine hours for #1 stay below 10,000, the gearbox input #4 exceeds the 10,000 standard hours. As the LF is based on loads and not on real damage the tractor does not necessarily show fatigue or failure for two reasons:

1 The k-exponent for the fictive Wöhler curve influences the weighting of single high loads in ratio to low loads. Increasing the k from 5 to ∞ weights all load classes equally. This shifts load factor focus more to operational states at lower loads than peak-based single events at high loads. Nevertheless concept of fatigue demands a k exponent.

2 Reference does not meet engineers reference load spectra for machine design. In this case the LF shows a crossing of the 10,000 standard operation hours without failure occurrence, because real references have different distribution or generally higher load levels. Once more, using the real reference load spectrum does not guarantee a failure at that moment when the 10,000 standard operation hours has been reached or exceeded, because engineers usually add safety factors on top to reduce the probability of failures.

The Wöhler curve provides the statistical probability of material or component failure, but can vary greatly for a single machine. Keeping this in mind, the LF have to be seen as a load indicator on assembly level.

Table 12: Resulting LF for different tractor scenarios. Overall LF is weighted: engine 35 %, gearbox input 15 %, gearbox output 15 %, front axle 15 % and rear axle 20 %.

Assembly	Scenario 1 Contractor	Scenario 2 Dairy	Scenario 3 Hog	Scenario 4 Cashcrop S	Scenario 5 Cashcrop L
Engine	0.21	0.20	0.89	1.03	0.70
Gearbox input	0.16	0.11	1.41	1.65	1.11
Gearbox output	0.04	0.08	5.54	5.79	4.21
Front axle	0.02	0.03	1.12	1.15	0.98
Rear axle	0.05	0.11	4.38	4.60	3.93
Overall *LF*	**0.12**	**0.12**	**2.46**	**2.64**	**2.02**

Further consolidation of the assembly-specific LF to one encompassing LF for the tractor is done by weighting the individual assembly LF by price. The ratio is shown in chapter 3.5.1. It is obvious that scenarios #3 - #5, which are mainly influenced by cash-crop applications such as tillage, show higher LF than scenarios #1 and #2. The tractor from the small cashcrop scenario shows the highest loads for each assembly because of the highest portion of heavy tillage work, while the tractor from scenario #1 (contractor) and #2 (dairy) show the lowest load factors.

LF for *engine* are relatively close together and span from 0.20 for dairy up to 1.03 for cashcrop small. Engine LF in scenario #4 are 5 times higher than loads of scenarios #1 and #2. Only scenario #3 and #4 reach or come close to 1.00 because all other scenarios stay below the reference load spectrum (see Figure 52). Scenario #5 shows medium loads because the load spectrum stays in between curves #1 - #4. The lowest engine load factor is observed for scenarios #1 and #2. Achieving a LF above 1.0 for the engine is almost impossible because the engine-ECU calculated output torque is cut off at the engine's maximum torque level.

On the *gearbox input* side, the situation is basically the same but the LF vary more. The lowest LF is achieved by #2 (dairy) with 0.11 and the highest by #4 (cashcrop small) with 1.65. Past loads for scenario #4 are almost 16 times higher than for scenario #2. Scenarios #1 and #2 show lower gearbox input load factors in comparison to engine output load factors while #3 - #5 show rising LF. This is because of the assumed high portion of PTO work in contractor and dairy applications (see Table 10). The rising LF for scenarios #3 - #5 is a result of dynamic effects during field operation which were measured on the gearbox input side, not the engine side. However the LF followed the engine output LF and maintained a relative advantage between the tractors.

The *gearbox output* side is mainly influenced by heavy pull applications such as grubbing or ploughing. These applications are not considered in scenarios #1 and #2 but play a big role in scenarios #3 - #5, which explains the large differences of 0.04 - 0.08 to 4.21 - 5.79. Past loads on drive wheel side of the gearbox show LF which are 100 times higher for the tillage-driven load spectra.

Front axle results are a bit closer looking at the LF but the range is still extensive. Scenario #1 ends at 0.02 while scenario #4 achieves 1.15. Nevertheless, the heavy tillage scenarios come close to the assumed reference: #3 1.12; #4 1.15; #5 0.98. Contractor and dairy tractors show a greater ratio of applications where front wheel assist is not engaged but passively driven and therefore only subjected to very low loads. In comparison to the front axle the *rear axle* reaches load factors from 3.93 to 4.60 for cashcrop large and cashcrop small scenarios. Again, the load factors reflect the visible grouping of the gearbox output load spectra #1, #2 and #3 - #5. When adding front axle and rear axle load factor, the resulting LF almost meets the gearbox output load factor. For scenarios #1 and #2, the previously described effects, such as recirculating power or forerunning of the front axle, exceed the low load factors so that this does not work under low load factor conditions.

For the *overall* tractor load factor, the whole tractor is evaluated by one load factor. Table 12 shows relatively low LF of 0.12 in the contractor and dairy scenario, which means that a tractor under these assumed conditions would be loaded only by 12 % in comparison to a standard reference tractor. In contrast cashcrop large show overall LF of 2.02 and cashcrop small LF of 2.64 which means that tractors under these assumed conditions would be subjected to a load of 264 % of a standard reference tractor. In other words, for 1 operation hour on the cashcrop large tractor, the smart tractor

meter would count 2.02 standard operation hours while it would count 0.12 standard operation hours for the contractor or dairy tractor.

The LF behave like their positioning in Figure 52 where scenarios #1 and #2 stay completely left of the reference load spectrum and scenarios #3 - #5 stay completely above. The extreme range between the different scenarios is one of the things which makes tractor design very complicated. While the average of all scenarios would perfectly fit the reference, single machines are far above or far below. Of course, most tractors show better mixed-applications scenarios but the basic problem stays the same.

4.3 Load ratio

In order to calculate a load factor, it is necessary to have a reference load spectrum which represents a standard operation hour. This reference load spectrum is difficult to find, sometimes impossible, especially when comparing tractors from different manufacturers. To avoid this problem but still evaluate different tractors in comparison to each other, the load ratio is used (see 3.5.2). The method of load ratio always compares the load sums of the tractors to one specific tractor. **Table 13** lists the resulting LR for different tractors in comparison to tractor E which is set as 1.0. Load sums are taken from the different scenarios #1 - #5. The PTO LR is also listed but is not considered in the overall LR calculation. The LR provides information about relative advantage or disadvantage of tractors in comparison to a reference tractor. The lower the resulting LR, the lower the past loads on the specific assembly or the whole tractor. This provides better transparency for tractors on the used market and indicates relative advantages to other tractors. Using the example of Table 13 tractor E is set as basis for the analysis. This causes all values to change to 1.0.

Engine LR of tractor A and B only show 24 % and 23 % of tractor E, respectively, while tractors C and D cumulated 153 % and 195 % of the engine load sum of tractor E, respectively. From an engine point of view, in comparison to tractor E, tractors A and B have a relative advantage, while tractors C and D have a relative disadvantage.

Table 13: Resulting LR for different tractor scenarios, related to tractor E. Overall LR is weighted: engine 35 %, gearbox input 15 %, gearbox output 15 %, front axle 15 % and rear axle 20 %. The scenarios are exemplary and equal the previously described application scenarios: #1 contractor, #2 dairy, #3 hog, #4 cashcrop small and #5 cashcrop large.

Assembly	**Tractor A**	**Tractor B**	**Tractor C**	**Tractor D**	**Tractor E**
	Scenario 1	Scenario 2	Scenario 3	Scenario 4	Scenario 5
Engine	0.24	0.23	1.53	1.95	1.00
Gearbox input	0.11	0.08	1.51	1.96	1.00
Gearbox output	< 0.01	0.01	1.74	2.33	1.00
Front axle	0.01	0.01	1.75	2.34	1.00
Rear axle	0.02	0.05	1.40	1.87	1.00
Rear PTO*	3.60	2.13	1.28	0.23	1.00
Overall *LR*	**0.10**	**0.10**	**1.57**	**2.06**	**1.00**

*) Not considered for overall LR calculation

The effect of high power consumption PTO implements is obvious when comparing engine and *gearbox input* load ratio. Tractors A and B have reduced values, but tractors C and D show increased values because most of the engine output torque was transferred to the gearbox and was used for pulling. The light used tractors A and B were only loaded with 8 % - 11 % of gearbox input load compared to tractor E, C and D, which ranged from 151 % - 196 % gearbox input load.

The range for *gearbox output* load ratio is even greater. While tractors A and B show values close to 0, tractors C and D are subjected to loads of 174 % - 233 % of tractor E. LR for the *front axle* is similar to gearbox output, but LR for the *rear axle* is slightly lower. The lack of any heavy pull applications for tractors A and B is seen in the rear axle LR of 2 % - 5 %. In contrast, tractors C and D cumulate 140 % - 187 % of the tractor's E load sum.

As mentioned above, *rear PTO* loads have a huge impact on the gap between engine output and gearbox input. In comparison to tractor E, tractor A achieves the highest LR at 360 %; tractor B at 213 % and tractor C at 128 %. Since PTO evaluation in terms of load factor was not possible because of missing reference load spectrum, it was not taken into account for LF calculation and for this reason is also not considered for the overall LR in Table 13.

When considering the complete tractor, the trend which already was apparent for assembly LR continues. Tractors A and B have the lowest overall LR and therefore the biggest relative advantage in comparison to tractor E. Tractors C and D both show higher load ratio than tractor E and for this reason have a relative disadvantage in comparison to tractor E.

Taking rear PTO LR of 10 % into consideration for overall tractor LR calculation and reducing all other assemblies by 2 %-points changes the resulting overall LR:

- Tractor A: 0.46
- Tractor B: 0.31
- Tractor C: 1.54
- Tractor D: 1.87

Overall LR of tractor A and B increase while C and D slightly decrease because of the less intense usage of the PTO. Tractor B now has the absolute advantage. But the assumed 10 % weighting for PTO LR is quite high compared to the remaining 28 % for the whole gearbox. For this reason it does not make sense to take PTO LR into calculation of overall tractor LR but it brings more transparency into the tractor's past.

Besides the relative advantage or disadvantage, using LR calculation can help a buyer to find a used tractor that fits their need more precisely. While a cashcrop farmer probably would look for good engine and gearbox condition, a dairy farmer who looks for a tractor for powering the fodder mixing trailer puts the focus on engine and PTO.

Because the method of load ratio counts and evaluates past machine loads independent from tractor size, age or operation hours, it can be used for direct comparison of tractors from different manufacturers, tractors of different age or different size. On the other hand, the LR only cumulates machine load but does not make any prediction of remaining lifetime.

5 TRANSFER-ASPECTS TO REAL APPLICATION

5.1 Simplification of measurement

To evaluate the potential of simplified measuring methods different aspects are discussed in the following chapter. Results from the calculation of average fuel consumption per hour, engine load by fuel load, engine load by time and engine load by revolutions are displayed in **Figure 54**. In addition, **Table 14** lists engine torque load by engine speed corrected fuel consumption from engine map.

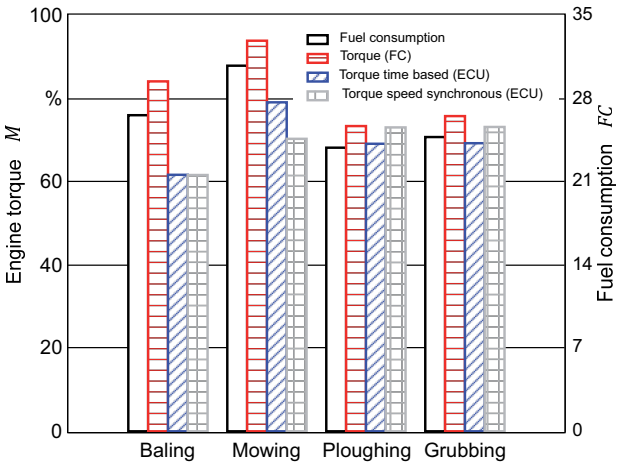

Figure 54: Comparison of engine load related parameters which were gathered from vehicle CAN-Bus.

Table 14 and Figure 54 show that overall fuel consumption for a tractor works well as an indicator for engine load as long as the engine operates at an optimal point in the engine map. For heavy-pull field operation like ploughing and grubbing, the engine transmission control unit sets the transmission ratio to the point of maximum torque which is in the range of 1,200 - 1,600 min^{-1}. Here the calculation of engine load by engine ECU results in 73.04 % engine torque and 73.37 % by fuel consumption. Taking average engine operation speed into account, shifts corrected engine torque to 69.17 % and 72.81 %, respectively. Results for grubbing are similar and show less

deviation between the simple calculation of engine torque by fuel consumption, the engine ECU calculated parameters and the results from the engine map.

Table 14: Comparison of alternative engine torque calculation methods, instead of strain gauge measuring.

	Ø Engine speed	Ø Engine torque load % nominal engine torque		
	min^{-1}	by ECU	by fuel consumption	by fuel consumption and average engine speed
Baling	1,949	61.77	81.91	78.49
Mowing	1,994	70.31	93.89	89.48
Ploughing	1,602	73.04	73.37	69.17
Grubbing	1,539	73.16	75.78	72.81

For constant engine speed applications such as baling or mowing, due to the need of a certain PTO speed, the engine runs at a less efficient point of the engine map. At this point output torque and fuel consumption do not match anymore. While real engine output torque for baling is 61.77 % of nominal torque, it is 81.91 % by fuel consumption. Taking the average engine operation speed into consideration, changes the engine torque load to 78.49 %. The offset stays the same as for torque calculated by fuel consumption. The same gap is shown in the analysis of the mowing application. This large offset of about 20 %-points comes from the fixed high engine speed which runs the engine at a point of high specific fuel consumption. Also the different engine controller strategy - fixed speed - causes the engine to use high injection rates to keep speed as close as possible to the engine target speed.

Another problem using the ECU calculated engine torque is that this system only provides positive torque within the range of 0 - 125% of engine nominal torque, as evident in **Figure 55**. While the ECU calculated load spectrum ends at 2 % frequency, the measured gearbox input side load spectrum shows single load peaks up to a relative frequency of 0.001 %. The highest ECU calculated torque is at 125 %, while measured torque goes up to over 180 % nominal torque. The slight shift between the ECU engine

torque curve and the strain gauge gear box input torque is a result of moderate losses by auxiliaries, already described in chapter 3.4.2.2.

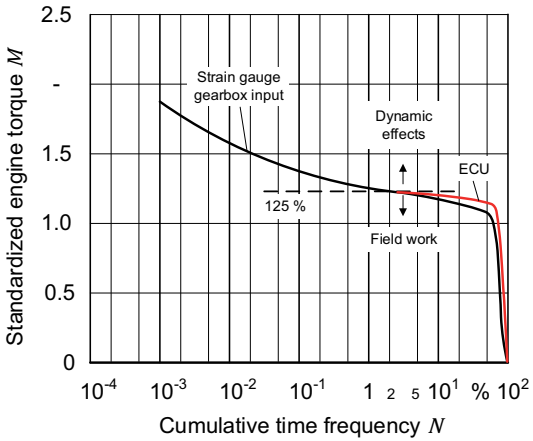

Figure 55: Comparison of ECU calculated engine output load spectrum and strain gauge measured gearbox input load spectrum for ploughing with a standard tractor. The dotted black line indicates 125 % engine torque, which is the maximum engine ECU calculated engine output torque.

The diagram in **Figure 56** shows measured gearbox output torque at the gearbox carrier shaft. Both curves, the strain gauge measured torque and the gearbox ECU calculated curve show good correlation, but the strain gauge measured torque stays about 10 % above the gearbox ECU calculated torque curve. Although the ECU calculated curve in **Figure 57** shows good reaction to effects within the drivetrain, the real strain gauge measurement detects higher peaks. The ECU calculates positive torque only. With the short negative peaks coming from subtraction of the front axle, it is not possible to distinguish between positive and negative torque when vehicle status changes from pull to push. This however is clearly detected by a strain gauge measurement.

Taking the data and analyses from this chapter into account, engine fuel consumption can be used as a basic indicator for general operation but does not meet the needs of

a load based tractor evaluation system because it does not consider effects from the environment or dynamic effects within the drivetrain.

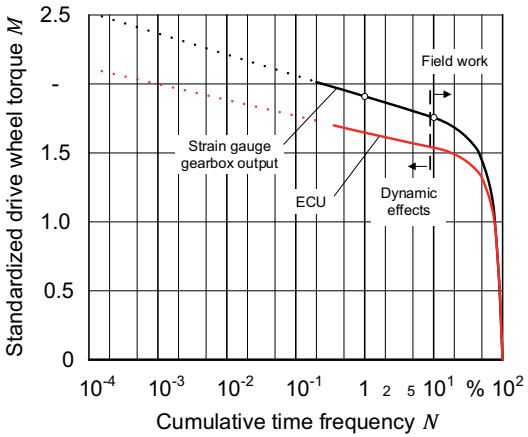

Figure 56: Comparison of ECU calculated gearbox output load spectrum and strain gauge measured gearbox output load spectrum for ploughing.

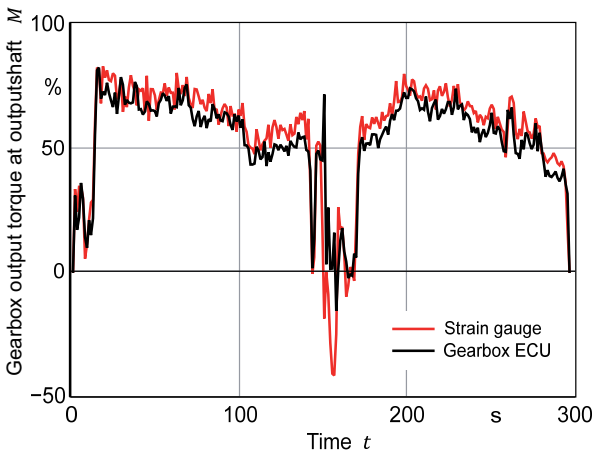

Figure 57: Comparison of ECU calculated and strain gauge measured gearbox output torque, sample rate 1 Hz.

5.2 Further optimization of the suggested method

The described method uses sensor data from the tractor drivetrain. This data is analyzed and evaluated under aspects of fatigue. In addition to the drivetrain, other components are also subjected to stress. A lot of components have structural functions, like the tractor frame, front and rear lift, engine, gearbox and axles. Some of them are evaluated by the described method under aspects of fatigue within the drivetrain, but not for *structural fatigue*. Modern tractors are equipped with acceleration sensors for the breaking system and gyroscopes for the steering systems. Electronically controlled front and rear lifts exert pressure in the lifting cylinders. Also, data from the front suspension could be used to detect forces and shocks which influence structural fatigue.

Single events do have serious impact on several components within a tractor. Engine start procedure at very low temperatures, engine stall due to PTO overload or overheating of hydraulic pumps can also cause severe damage and should also be considered. The presented method does not take these single events into account because it is very difficult to evaluate them without specific data and knowledge. Nevertheless, these single events should at least be detected and recorded additionally for further qualitative tractor evaluation.

The tractor lifetime load spectra were *scaled up* to the common expected lifetime of 10,000 h. Real measurements for the application load spectra are between 5 - 50 h. Experience shows that load spectrum characteristics stay very stable after 2 hours of measurement, but single peak events at the area of high torque usually do not occur during the measurement period. For this reason, load spectrum for different applications could show load peaks left from the last point and for this reason result in higher load factors or load ratio than in the presented analysis.

Pseudo damage calculation was used to compare tractor lifetime load spectrum to reference load spectrum. The quality of the results depends on the quality of the reference load spectra used. The author adapts published load spectra because of a lack of other sources but it would be better to take the load spectra which was used for the tractor design instead.

The test tractor was equipped with additional, expensive and fragile strain gauge sensors which are not available for tractor series production. Load assumption can be done based on calculated engine torque and calculated gearbox torque by ECUs but

does not satisfy all demands because this procedure does not take external effects into account. For this reason, further research on the field of affordable and robust torque sensors for tractor series production is necessary. Interesting approaches were published by Wieckhorst et al. [90].

All data was stored on the tractor data logger on the machines and was analyzed later manually. A series system should ideally use telemetry to transfer the data from the machines all over the world to a server where the data storage and analysis is done.

Nevertheless, the described method shows the potential of a more transparent and more precise evaluation method of tractors. It allows the evaluation of a tractor in an objective way based on past, real machine loads instead of counting operation hours which is state of the art nowadays. The two aspects of load factor and load ratio can help in specific ways.

5.3 Looking forward

Today tractors are evaluated by their manufacturing year, operation hours and visual condition. While machines such as combines or forage harvesters store additional data like hectares harvested, engine and process hours, plus more detailed information such as hours straw chopper in usage, common tractors simply have a lack of information, although tractors are the most commonly used piece of agricultural equipment. As shown in Figure 39 and Figure 40, application-type varies over the year and depends highly on farm size, farm type and many other factors. It is almost impossible to estimate real tractor usage and even harder to estimate real tractor loads because these vary greatly, as shown in Figure 52.

The presented method can fulfill these demands and make tractor load history more transparent. This provides both, the customer and the manufacturer with better information and increases the knowledge base for them. A telemetry-based system can be used to record and analyze tractor load spectra at the assembly level. Knowing loads of the entire tractor fleet helps to promote more precise tractor development. Nowadays some tractors are equipped with sensors and are sent to test farms. Based on

the results gathered from these tractors, the lifetime load spectra are generated. Unfortunately, this is not as precise as knowing load data from the entire global tractor fleet.

During tractor field validation, where pre-series machines are sent to test customers all over the world (which is a costly procedure), occurring damages can be related to the achieved load factor. This procedure would be even more interesting, when the internal load spectra, that were used for tractor design are set as reference load spectrum. By checking the individual load factor of a tractor, it becomes obvious if the tractor is subjected to a load greater than the manufacturer originally assumed or recommended (LF > 1.0) or if test objectives are not fulfilled (LF < 1.0).

Product portfolio can be optimized based on load factors. For example regions with very high loads on specific assemblies due to local conditions are equipped with heavy duty components or the flagship models of a series, which are technically already at the cutting-edge, are not taken into the regional product portfolio.

On the second hand market customers frequently fail to evaluate the object of purchase correctly because of an information asymmetry [10]. By means of LF or LR customers have more transparency about a tractor's history and get precise information about real loads on the different assemblies.

The described method can be used as indication for individual tractor maintenance intervals. Nowadays engine or gearbox oil change is done equally on a timely basis, but the loads vary a lot as shown. Based on load information, maintenance intervals can be shortened or enlarged to fit customers individual machine load behavior. This reduces cost of operation and guarantees a high uptime rate.

6 CONCLUSION

Tractors face varying loads depending on farm type and size, geographical location, and many other factors. Nevertheless, tractors are evaluated by operation hours which do not consider these varying loads [91]. Customers and tractor manufacturers need more transparency in tractor usage and past loads. Condition monitoring is an approach which can help to fulfill these needs but adds additional costs to the tractor. There is a demand for an assembly-level-method to evaluate tractors based on their real loads.

To this end, a test tractor was equipped with strain gauges to measure torque flow within the drivetrain. Application-specific load spectra were classified speed-synchronous and scaled to a tractor lifetime load spectrum for each assembly. Different scenarios were generated by choosing the applications founded on typical farm types. By means of a pseudo damage-calculation method the tractor lifetime load spectra were compared to common reference load spectra [12; 36]. These were adapted to the different characteristics of CVT tractors and were set as reference operation hour. A hypothetical Wöhler curve was introduced for weighting of load level in belongings of damage contribution.

The resulting load factors show a wide range between the different scenarios. While some assemblies, such as the engine, result in load factors between 0.20 - 1.03 (which already display extreme differences), others, like the gearbox output, generate load factors from 0.11 - 4.60. The load factor relates the measured tractor lifetime load spectrum to a reference load spectrum, which is considered to be the lifetime average load spectrum of 1 standard operation hour. Taking the load factor of 0.20 for the engine means 1 operation hour will equal 0.20 standard operation hours.

Because a valid reference load spectrum is needed for load factor calculation, a load ratio is introduced. This compares directly the calculated load sums of the tractors and gives an indication of the relative advantage of a tractor in comparison to another tractor can be used. This helps to evaluate tractors from different manufacturers. Both methods meet specific demands and the results show that the qualitative statement is not changed by choosing one or the other variant of the method.

Knowledge about the actual torque within the tractor drivetrain is necessary for this method, but current series-production tractors are not equipped with such sensors. For

this reason, an analysis was done to determine if the method works without the strain gauge sensors by calculation of torque, based on engine ECU torque output and gearbox ECU torque output. The results show that a basic indication can be given but it does not register load peaks which are caused by external effects and torque split between front and rear axle changes dynamically during field operation. This makes a statement regarding axle load impossible.

The described method evaluates tractor loads but does not calculate tractor damage or remaining lifetime. An indication into these directions is not possible because first of all, precise damage calculation requires knowledge of the components' Wöhler curve and second of all it only gives a statistical probability of failure. This means that although failure is predicted, the tractor does not necessarily fail. This reduces the method's credibility. The calculation of remaining-lifetime is even more inaccurate because in addition to the uncertainty of damage calculation, future tractor usage must be predicted, which is not possible to do with precision.

This method offers better knowledge about machine usage and resulting loads for tractor manufacturers and can also help customers on the used-machinery market to get more transparency about past machine loads. Manufacturers can design future machines more precisely due to a better knowledge of load spectra, furthermore tractor validation can be done based on the resulting load factor. Regional product adaptations for specific high load demands can be done to increase durability. Failures during product validation can be related to the actual assembly load factor and help to evaluate the importance of individual failures.

Load-based evaluation of tractors has great potential, but further research in the field of robust and simple torque sensors for series application should be done. A next step to make the method more comprehensive might be to take structural loads and single events such as engine cold starts or engine stalls into consideration.

7 REFERENCES

[1] Dörpmund, H.-G. and B. Anders Lützen: Der Traktor muss zum Job passen. Lohnunternehmen 72 (2017) No. 3, pp. 20-22.

[2] Balbach, F.: Lastkollektive von Ackerschlepper-Motoren bei unterschiedlichen Feldeinsätzen in verschiedenen Regionen. Bachelor thesis, 2013, University of Hohenheim, Stuttgart, Institute of Agricultural Engineering, unpublished.

[3] • Boog, M.: Steigerung der Verfügbarkeit mobiler Arbeitsmaschinen durch Betriebslasterfassung und Fehleridentifikation an hydrostatischen Verdrängereinheiten. Dissertation Karlsruhe Institut of Technology, 2010, Karlsruher Schriftenreihe 4: Fahrzeugsystemtechnik. Karlsruhe: KIT Scientific Publishing 2010.

[4] Brinkschulte, L. and M. Geimer.: Echtzeitfähige Abschätzung der Restlebensdauer von Komponenten, ATZoffhighway 10 (2017) No. 3, pp. 54-61.

[5] -,-: Schlepper-Bundesliga. PROFI, https://www.profi.de/news/Schlepperbundesliga_138.html, 18.12.2017.

[6] -,-: Written notice, VDMA Agricultural Machinery, 17.03.2018

[7] -,-: Genesis database, Federal Statistical Office Germany (DESTATIS), www.destatis.de/genesis, 16.03.2018.

[8] -,-: Fahrzeugzulassungen (FZ 20) - Neuzulassungen und Besitzumschreibungen von Nutzfahrzeugen 2011 - 2016, Federal Motor Transport Authority Germany (KBA), https://www.kba.de/DE/Service/Downloads/downloads_node.html, 16.03.2018.

[9] • Renius, K.-T.: Traktoren und Erdbaumaschinen. Lecture notes, Technical University of Munich, 2012.

[10] Akerlof, G.A.: The market for "Lemons": quality uncertainty and the market mechanism. The Quarterly Journal of Economics 84 (1970) No. 3, pp. 488-500.

[11] Renius, K.-T.: Trends in tractor design with particular reference to Europe. Journal of Agricultural Engineering Research 57 (1994) No. 1, pp. 3-22.

[12] • Renius, K.-T.: Last- und Fahrgeschwindigkeitskollektive als Dimensionierungsgrundlagen für die Fahrgetriebe von Ackerschleppern. Düsseldorf: VDI-Verlag, 1976.

[13] Welschof, G.: Entwicklungslinien im Schlepperbau: Kriterien für die heutige und zukünftige Entwicklung, Grundlagen der Landtechnik 24 (1974) No. 1, pp. 6-13.

[14] • Radaj, D.: Ermüdungsfestigkeit. Berlin/Heidelberg: Springer-Verlag, 2003.

[15] -,-: DIN 3990/6: Tragfähigkeitsberechnung von Stirnrädern - Betriebsfestigkeits-rechnung. Berlin: Beuth-Verlag, 1994.

[16] • Haibach, E.: Betriebsfestigkeit: Verfahren und Daten zur Bauteilberechnung. Berlin/Heidelberg: Springer-Verlag, 2006.

[17] Miner, M.A.: Cumulative damage in fatigue. Journal of Applied Mechanics 12 (1945) No. 3, pp. 159-164.

[18] • Schaller, K.V.: Betriebsfestigkeitsuntersuchungen zur Grübchenbildung an einsatzgehärteten Stirnradflanken. Dissertation Technical University of Munich, 1990.

[19] • Suchandt, T.: Betriebsfestigkeitsuntersuchungen zur Zahnfußtragfähigkeit einsatzgehärteter Zahnräder und zur Bruchfestigkeit vergüteter Laschenketten. Dissertation Technical University of Munich, 1994.

[20] • Hoffmann, K.: Eine Einführung in die Technik des Messens mit Deh-nungsmeßstreifen. Darmstadt: Hottinger-Baldwin-Meßtechnik-GmbH 1987.

[21] • Giesecke, P.: Dehnungsmeßstreifentechnik: Grundlagen und Anwendungen in der industriellen Meßtechnik. Braunschweig: Vieweg 1994.

[22] -,-: Coupling Inductive Sensor Telemetry. Firmenschrift COUPLER_KATALOG.odr.//20170603, Manner Sensortelemetrie, Spaichingen, 2017.

[23] Renius, K.-T.: Betriebsfestigkeitsberechnungen von Maschinenelementen in Ackerschleppern mit Hilfe von Lastkollektiven. Konstruktion 29 (1977) No. 3, pp. 85-93.

[24] Biller, R.H.: Ermittlung von Gesamt-Lastkollektiven für Ackerschlepper. Grundlagen der Landtechnik 31 (1981) No. 1, pp. 16-22.

[25] Renius, K.-T.: Betriebsfestigkeitsberechnung und Laborerprobung von Zahnrädern in Ackerschleppergetrieben. VDI-Berichte (1979) No. 332. pp. 225-234.

[26] Lüpfert, U.: Ermittlung und Anwendung von Lastkollektiven im Traktorbau. Grundlagen der Landtechnik 23 (1973) No. 1, S. 7-10.

[27] Kloth, W. and T. Stroppel: Kräfte, Beanspruchungen und Sicherheiten in den Landmaschinen. Zeitschrift des Vereins Deutscher Ingenieure 80 (1936) No. 4, pp. 85-92.

[28] Wilmer, H.: Schön gemacht: Deutz-Fahr 6160.4 TTV. Profi (2014) No. 6, pp. 12-19.

[29] Momal, P.: Verbal message, Company CLAAS Tractor SAS, Advanced-Development, 30.06.2016.

[30] • Pichlmaier, B.: Traktionsmanagement für Traktoren. Dissertation Technical University of Munich, 2012.

[31] Gerlach, A.: Über die Kräfte in Zahnradgetrieben von Schleppern. Grundlagen der Landtechnik 6 (1956) No. 7, pp. 107-110.

[32] • Coenenberg, H.-H.: Zum Verhalten der Kupplung und ihrem Einfluss auf die Schwingungs- und Spitzenbeanspruchungen im Fahrzeugtriebwerk, speziell Schleppertriebwerk. Dissertation Technical University Braunschweig, 1963.

[33] Coenenberg, H.-H.: Die Belastungen von Motor, Fahrgetriebe und Zapfwelle bei Ackerschleppern: Zur Analyse ihrer Häufigkeitsverteilungen. Grundlagen der Landtechnik 13 (1963) No. 16, p. 16-30.

[34] • Steinkampf, H.: Betriebseigenschaften von Ackerschlepperreifen bei unterschiedlichen Einsatzbedingungen. Dissertation Technical University Braunschweig, 1996, Wissenschaftliche Mitteilungen der Bundesforschungsanstalt für Landwirtschaft (FAL) No. 80. Braunschweig-Völkenrode 1986.

[35] Kühlborn, H.: Aufnahme und Auswertung von Belastungsverläufen in Schleppertriebwerken. Landtechnische Forschung 19 (1971) No. 3, pp. 65-71.

[36] Meiners, H.-H.: Die Beanspruchung einzelner Schlepperaggregate bei unterschiedlichen landwirtschaftlichen Arbeiten. Landtechnik 39 (1984) No. 10, pp. 438-441.

[37] Biller, R. H.: Zur Belastung der Schlepperzapfwelle bei unterschiedlichen Arbeitseinsätzen. Landtechnik 38 (1983) No. 11, pp. 470-473.

[38] -.-: CLAAS AXION 950 CMATIC. DLG e.V. Testzentrum Technik und Betriebsmittel, http://www.dlg-test.de/pbdocs/traktoren/CLAAS_AXION_950.pdf, 21.03.2017.

[39] Denkena, B.; J. Berger and P. Blümel: Instandhaltung mit nichtlinearer Dynamik. Werkstatttechnik online 93 (2003) No. 10, pp. 710-714.

[40] • Coronado, D. and K. Fischer: Condition monitoring of wind turbines: state of the art, user experience and recommendations. Bremerhaven, Fraunhofer IWES Project Report 2015.

[41] -.-: Manual ARION 650-640-630-620 CMATIC ARION 550-540-530 CMATIC company publication 00 2243 252 1 04/2016, CLAAS KGaA mbH, 2016.

[42] Buhrmester, J.: Fendt 939 Vario S4. DLG e.v., http://www.dlg-test.de/tests/6297.pdf, 23.03.2017.

[43] Emmelheinz, J.: Remote Services sind ein Zukunftsthema, ETR (2012) No. 12, pp. 102.

[44] Gladieux, S.: Achieving optimum mobile mining equipment performance through remote condition monitoring. International VDI Conference, 10.-

11.05.2016 Ulm. In: Connected Off-Highway Machines. Presentation document VDI Wissensforum 2016.

[45] Brown, M.V.: Applying the predictive approach to maintenance. TheNEWS, http://www.achrnews.com/articles/90029-applying-the-predictive-approach-to-maintenance, 16.03.2016.

[46] Agoston, A.; C. Schneidhofer; N. Dörr and B. Jakoby: A concept of an infrared sensor system for oil condition monitoring. e & i (electrotechnology and information technology) 125 (2008) No. 3, pp. 71-75.

[47] Antoniadou, I.; G. Manson; W.J. Staszewski; T. Barszcz and K. Worden: A time-frequency analysis approach for condition monitoring of a wind turbine gearbox under varying load conditions. Mechanical Systems and Signal Processing 64-65 (2015) pp. 188-216.

[48] • Köhler, M.; S. Jenne; K. Pötter and H. Zenner: Zählverfahren und Lastannahme in der Betriebsfestigkeit. Berlin/Heidelberg: Springer-Verlag 2012.

[49] Nie, M. and L. Wang: Review of condition monitoring and fault diagnosis technologies for wind turbine gearbox. Procedia CIRP 11 (2013), pp. 287-290.

[50] Tchakoua, P.; R. Wamkeue; M. Ouhrouche; F. Slaoui-Hasnaoui; T. Tameghe and G. Ekemb: Wind turbine condition monitoring: State-of-the-art review, new trends, and future challenges. Energies 7 (2014) No. 4, pp. 2595-2630.

[51] Botsaris, P.N. and J.A. Tsanakas: State-of-the-art in methods applied to tool condition monitoring (TCM) in unmanned machining operations. The international conference of COMADEM, 11.-13.6.2008 Prague. In: Proceedings of the international conference of COMADEM 2008, pp. 73-87.

[52] Halme, J.: Condition monitoring of a material handling industrial robot. COMADEM 12.-15.6.2006 Luleá, Sweden. In: Proceedings of the 19th international conference of COMADEM 2006.

[53] -,-: DIN ISO 10816-3:Mechanische Schwingungen - Bewertung der Schwingungen von Maschinen durch Messungen an nicht-rotierenden Teilen - Teil 3:

Industrielle Maschinen mit einer Nennleistung über 15 kW und Nenndrehzahlen zwischen 120 min-1 und 15,000 min-1 bei Messungen am Aufstellungsort. Berlin: Beuth-Verlag, 2009.

[54] • Witzig, J.: Flankenbruch - Eine Grenze der Zahnradtragfähigkeit in der Werkstofftiefe. Dissertation Technical University of Munich, 2012. Volume Engineering Science: Munich: Verlag Dr. Hut 2012.

[55] Schools, T.: Condition monitoring of critical mining conveyors. Engineering and Minig Journal (2015) No. 3, pp. 1-3.

[56] -,-: ICE-Unfall von Eschede. Wikipedia (Wikimedia Deutschland e.V.), https://de.wikipedia.org/wiki/ICE-Unfall_von_Eschede, 23.03.2017.

[57] Dawson, B.: Derailed: System failure case Studies. NASA - System Failure Case Studies 1 (2007) No. 5, pp. 1-4.

[58] Ho, S.L.; K.K. Lee; K.Y. Lee; H.Y. Tam; W.H. Chung; S.Y. Liu; C.M. Yip and T.K. Ho: A comprehensive condition monitoring of modern railway. International conference on railway condition monitoring, 29.-30.11.2006 Birmingham, UK. In: The institution of engineering and technology - International conference on railway condition monitoring. London: The Institution of Engineering and Technology, pp. 125-129.

[59] Tsunashima, H.; Y. Naganuma; A. Matsumoto; T. Mizuma. and H. Mori: Condition monitoring of railway track using in-service vehicle. In: Reliability and Safety in Railway. Rijeka, Croatia: InTech 2012, pp. 333-356.

[60] • Kolerus, J. and J. Wassermann: Zustandsüberwachung von Maschinen. Renningen: expert Verlag 1986.

[61] Klanfar, M.: Fuel consumption and engine load factors of equipment in quarrying of crushed stone. Tehnicki vjesnik - Technical Gazette 23 (2016) No. 1, pp. 163-169.

[62] Ryken, M. J. and J. L'Heureux: Understanding customer duty cycle through JDLink. VDI/MEG-Tagung Landtechnik 8.-9.11.2013 Hannover. In: VDI-Berichte No. 2193. Düsseldorf: VDI-Verlag 2013.

[63] -,-: The Carfax Vehicle History Report, CARFAX Europe GmbH, https://www.carfax.eu/sample-report, 27.04.2016.

[64] -,-: Fahrzeugmanagement - Manual, Daimler Fleetboard GmbH, http://www.fleetboard.com/portal/static/manuals/fzm/de_DE/Vehiclemanagement_Manual_DE.pdf, 03.11.2016.

[65] Bourauel, F.; H. Mühlberger; E. Starmühler; W. Weishaupt and P. Flohr: Service-Intervall-Anzeigevorrichtung für Kraftfahrzeuge. German patent application. DE 3104174 A1, 02.02.1989.

[66] Peters, S.: Großdieselmotor und Verfahren zum Betreiben desselben. German Patent Application. DE 102006046157 A1, 28.09.2006.

[67] Hoffmann, F. and R. Schmidt: Vorrichtung und Verfahren zur Ermittlung eines Verschleißkennwerts einer Brennkraftmaschine. German patent application. DE 10349875 A1, 25.10.2005.

[68] Urban, P.: Auswertungsverfahren zur Bestimmung des Schädigungsgrades einer Maschine oder Maschinenkomponente. German patent application. DE 19944435 A1, 16.09.1999.

[69] Oberg, J.; D. Pickert and V. Schumacher: Kontrollverfahren für die Wartung eines Kraftfahrzeuges. German patent application. DE 10029634 A1, 15.06.2000.

[70] Rice, T. D.; C.G. Janasek; K.K McKinzie. and D.J. Ziskovsky: Arbeitszyklusaufzeichnungssystem und Verfahren zum Schätzen des Schadens und der verbleibenden Lebensdauer von Antriebsstrangkomponenten. German patent application. DE 102015214357 A1, 29.07.2015.

[71] -,-: Telemetrie unter der Lupe: Was die Kurven verraten. Motorsport-Total, http://www.motorsport-total.com/f1/news/2014/08/telemetrie-unter-der-lupe-was-die-kurven-verraten-14080905.html?wing=2, 08.11.2016.

[72] -,-: Sicherung genetischer Diversität beim Rothirsch in der Kulturlandschaft. Büsgen-Institute University of Göttingen, http://www.wildbiologie-institut.de/index.php/de/downloads/category/5-rotwildtelemetrie?download=32:poster-gen-vielfalt, 08.11.2016.

[73] -,-: SNOWsat - Professionelles Pisten- und Flottenmanagement mit Schneetiefenmessung. Kässbohrer Geländefahrzeug AG, http://www.pisten-bully.com/fileadmin/content_pistenbully/modul_8_download/pistenbully_snowsat_09_2014_de.pdf, 08.11.2016.

[74] -,-: FUSE. AGCO GmbH, http://www.fendt.com/de/assets/article/4168/229231_Fuse_Broschuere_Deutsch_2015.pdf, 07.11.2016.

[75] -,-: Präzisionslandwirtschaft mit New Holland. New-Holland (CNH Industral N.V.), http://d3u1quraki94yp.cloudfront.net/nhag/eu/de-de/assets/pdf/plm/precision-land-management-brochure-germany-de.pdf, 07.11.2016.

[76] -,-: EASY - Efficient Agriculture Systems. CLAAS KGaA mbH, http://www.claas.de/blueprint/servlet/blob/896790/8325c172a9ce4a75a7d9dc3815caefa8/274858-dataRaw.pdf, 07.11.2016.

[77] Maehler, R.: Verbal message, Company CLAAS CES GmbH, product manager Telematics, 09.11.2016.

[78] Murakami, T.; T. Saigo; Y. Ohkura; Y. Okawa and T. Taninaga: Development of vehicle health monitoring system for large-sized construction machine. Komatsu Technical Report 48 (2002) No. 150, pp. 15-21.

[79] Fedde, T.: Verbal message, Company CLAAS Tractor SAS, head of advanced development, 12.02.2016.

[80] Reith, S.; J. Frisch and B. Winkler: Revision of the working time classification to optimize work processes in modern agriculture. Chemical Engineering Transactions 58 (2017).

[81] Winkler, B. and J. Frisch: Weiterentwicklung der Zeitgliederung für landwirtschaftliche Arbeiten. 19. Arbeitswissenschaftliches Kolloquium des VDI-MEG Arbeitskreises Arbeitswissenschaften im Landbau, 11.-12.03.2014 Dresden. In: Bornimer Agrartechnische Berichte No. 83. Potsdam-Bornim/Dresden: ATB Leibniz-Institut für Agrartechnik Potsdam-Bornim e.V., pp. 14-21.

[82] • Lalanne, C.: Mechanical vibration and shock analysis. London/Hoboken, N.J.: 2009.

[83] -,-: ISO 6336: Calculation of load capacity of spur and helical gears. Geneva: International Organization of Standardization, 2006.

[84] Blumöhr, T.; H. Zepuntke and D. Tschäpe: Die Klassifizierung landwirtschaftlicher Betriebe: Gemeinschaftliches Klassifizierungsverfahren in Deutschland. Wirtschaft und Statistik 6 (2006) No. 5, pp. 516-526.

[85] -,-: Verfahrensrechner Pflanze. Kuratorium für Technik und Bauwesen in der Landwirtschaft, http://daten.ktbl.de/vrpflanze/home.action, 17.10.2017.

[86] Rennert, R.; E. Kullig; M. Vormwald; A. Esderts and D. Siegele: FKM-Richtlinie Rechnerischer Festigkeitsnachweis für Maschinenbauteile. Frankfurt am Main: Forschungskuratorium Maschinenbau, 2012.

[87] W. Söhne: Beitrag zur Mechanik des Systems Fahrzeug-Boden unter besonderer Berücksichtigung der Ackerschlepper. Grundlagen der Landtechnik 13 (1963) No. 17, pp. 5-16.

[88] M. Dwyer: Prediction of drawbar test performance. Journal of Terramechanics 24 (1987) No. 2, pp. 169-177.

[89] -,-: DLG Powermix App. DLG e.V. Testzentrum Technik und Betriebsmittel, http://www.dlg-test.de/powermixapp/, 18.12.2017.

[90] Wieckhorst, J.; T. Fedde; L. Frerichs and G. Fiedler: Integrated measurement of tire soil parameters for tractors. VDI/MEG-Tagung Landtechnik, 06.-07.11.2015 Hannover. In: VDI-Berichte No. 2251. Düsseldorf: VDI-Verlag 2015, pp. 219-226.

[91] Balbach, F.; E. Nacke and S. Böttinger: Method for load-based evaluation of machines using the example of a tractor. VDI/MEG-Tagung Landtechik, 10.-11.11.2017 Hannover. In VDI-Berichte No 2300. Düsseldorf: VDI-Verlag 2017, pp. 521-528.